Microstructural landscape and vortex pinning scenarios in REBCO coated conductors prepared at high growth rates

Xavier Obradors

Teresa Puig, Joffre Gutiérrez

Institut de Ciència de Materials de Barcelona, ICMAB-CSIC, Catalonia, Spain

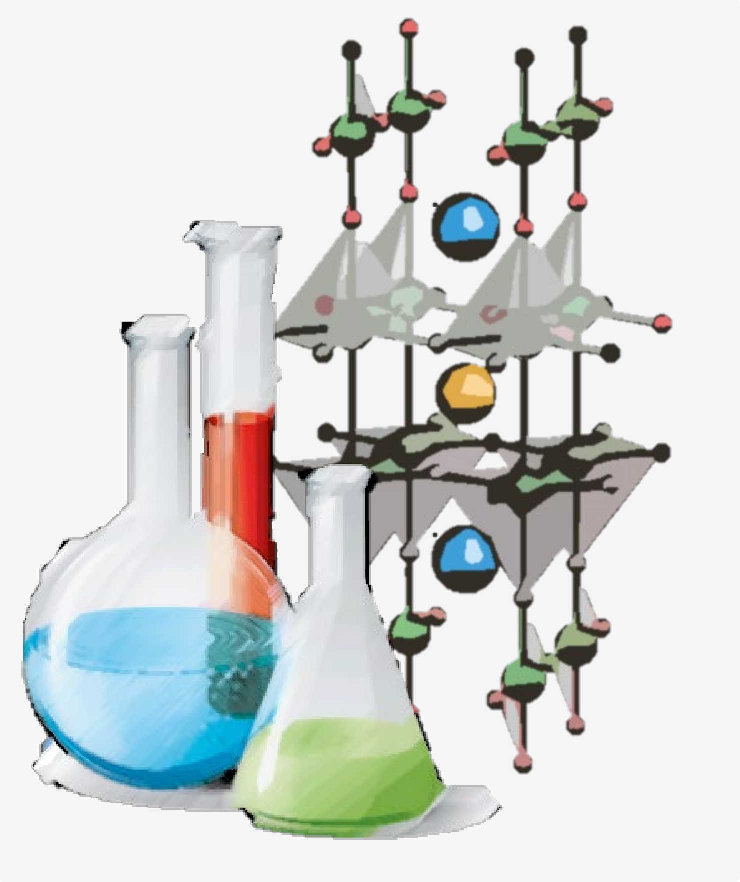

IRradiation Effects on HTS for Fusion

Motivation and outline

- Excepcional properties of REBCO Coated conductors at ultrahigh magnetic fields: excellent opportunity for compact fusion

- UHF magnets (20 T / 20 K) for fusion require extremely long lenghts of CCs (~ 20.000 km/magnet) with high performance (I_c (20T, 20 K))

- High throughput production of CCs is essential to cope with the expected demands: High growth rates of CCs need to be developed

- Understanding the impact of high growth rates on the microstructure and vortex pinning mechanisms of CCs is essential to optimize the potential of CCs

- Reliable methodologies to analyse the influence of high energy neutron irradiation in CCs are required

- Overview of vortex pinning scenarios of CCs prepared at high growth rates

REBCO coated conductors: enabling a new era of fusion energy

ICMAB INSTITUT DE CIÈNCIA DE MATERIALS DE BARCELONA EXCELENCIA SEVERO OCHOA

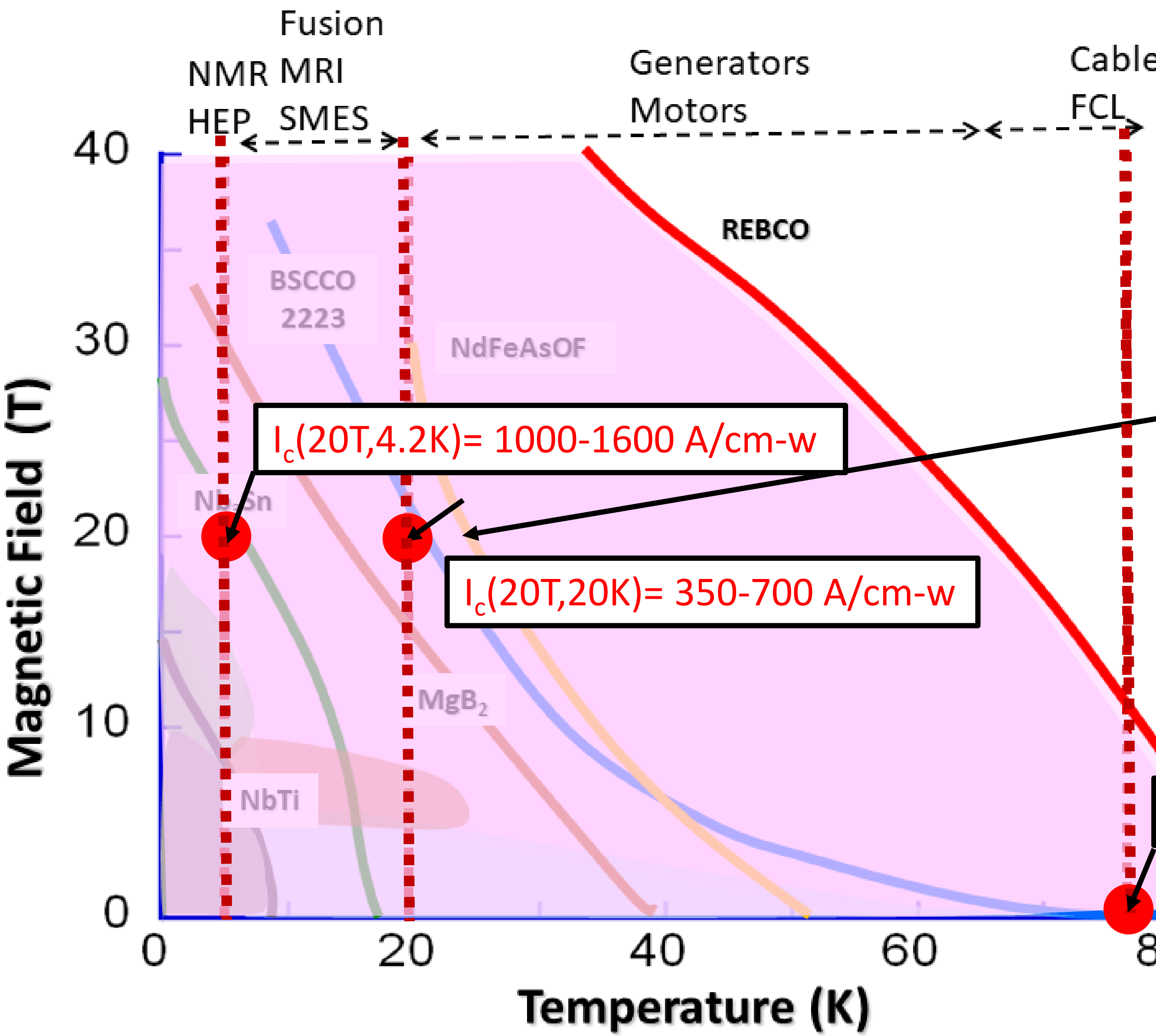

REBCO
COATED CONDUCTORS

"The highest Field with the lowest cryogenic cost"

MATERIALS SCIENCE

The prospects of high-temperature superconductors

Overcoming cost barriers could make high-temperature superconductors pervasive

By **Alexander Molodyk**[1] and **David C. Larbalestier**[2]

Science **380**, 1220, 2023

"...the present outlook for high-temperature superconductor materials and their industrial applications is historic..."

COMPACT FUSION

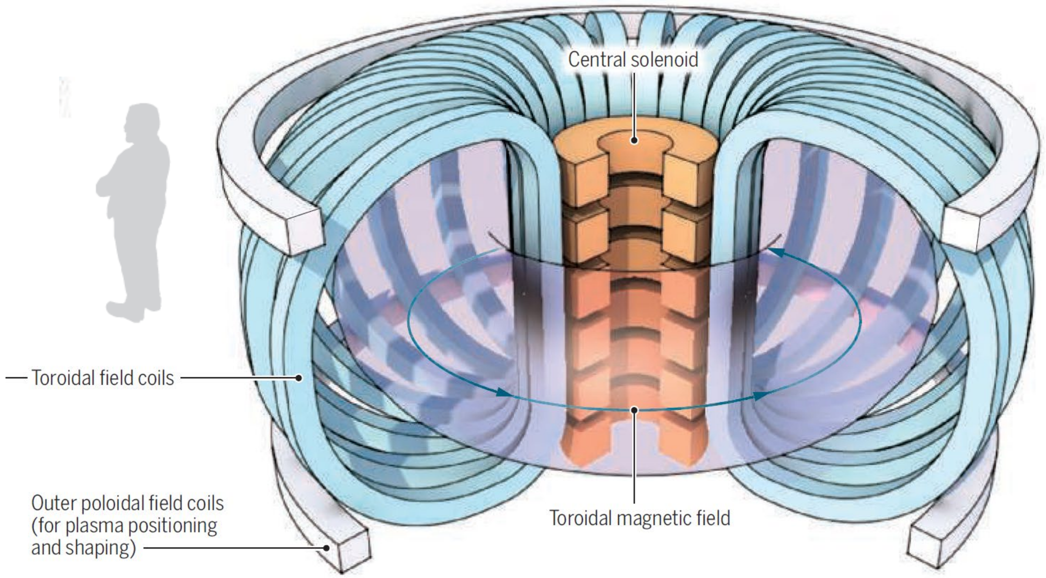

The applied superconductivity community is anticipating the virtuous cycle of price reduction and further demand from other electrotechnology applications that are not yet economic at today's REBCO CC prices

The development of compact nuclear fusion power generation is the immediate stimulus that has driven exponential annual volume increases.

Coated Conductors: materials objectives

Coated Conductor penetration € / kA m

CHEAPER

$$\frac{C}{P} = \frac{€}{G\ x\ L\ x\ W\ x\ J_c}$$

- Ultrafast growth (G)
- Lower capital investment (€)
- Larger area manufacturing (W, L)
- Higher throughput
- Simpler processing
- Simpler architecture
- Higher yield

BETTER

- Higher performance: $J_c(B, T)$
- Thicker REBCO films
- More robust
- Customized for Applications
- Thinner substrates (J_E)
- Nanostructure control: APCs
- Lower ac losses

Fast growth rate ⟷ Best combination ⟷ Nanocomposites

REBCO growth processing: simultaneous and sequential

MICMAB INSTITUT DE CIÈNCIA DE MATERIALS DE BARCELONA EXCELENCIA SEVERO OCHOA

Vapour-solid transformation | solid-solid gas mediated | Liquid-solid

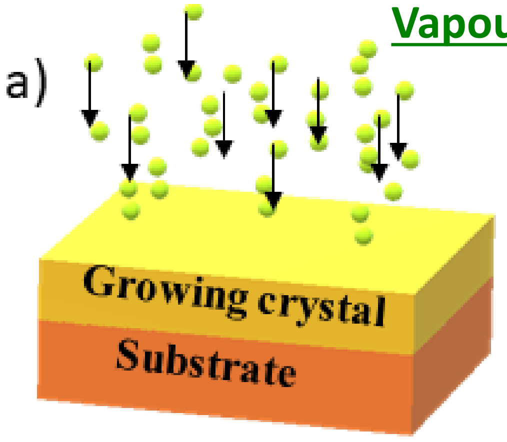

Growth from **vapour phase**
PLD, MOCVD, ME, MBE, Sputt

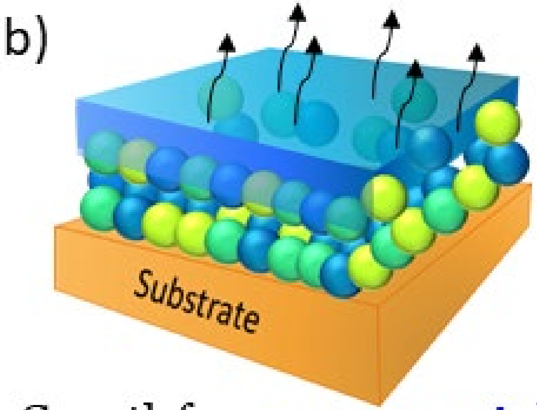

Growth from **nanocrystalline solids**
TFA-MOD, BaF_2

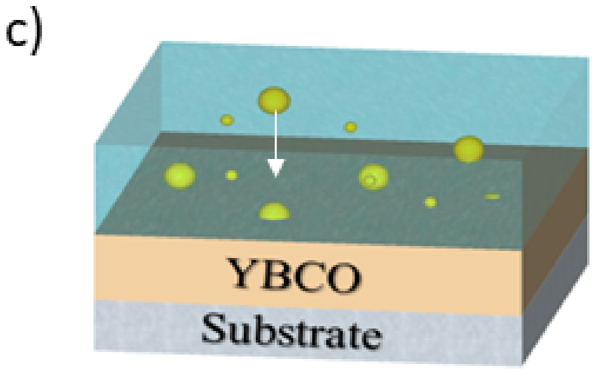

Growth from **liquid phase**
TLAG-CSD, RCE-DR, HLPE, VLS

Supersaturation, σ, is the driving force for crystallization: **$\sigma \propto G$** (growth rate)

$\sigma = (P_{ad} - P_{ad,e}) / P_{ad,e}$

Deposition rate
High vacuum environ.
Simultaneous

$P_{ad,e}$ = ad-atoms equilibrium pressure at surface growth front
P_{ad} = ad-atoms pressure at surface growth front

$\sigma = f\,(\ln (P_{HF}^2 / P_{H2O}))$

P_{HF} = HF partial pressure
P_{H2O} = water partial pressure
Sequential

$\sigma = (C_\delta - C_e) / C_e$

RE solubility,
Ba-Cu-O liquid

C_e = RE equilibrium concentration in the liquid
C_δ = RE actual concentration
Simultaneous or sequential

Growth rate: **G= 0.5-25 nm/s** | **G= 0.5-5 nm/s** | **G=10-1000 nm/s**

T. Puig, J. Gutiérrez, X. Obradors Nat Rev Phys (2023, doi.org/10.1038/s42254-023-00663-3); J. Driscoll et al, Nat Rev Mat (2021)

Transient Liquid Assisted Growth (TLAG)

European Research Council
Executive Agency

A new high throughput non-equilibrium kinetically controlled growth process

CSD
L. Saltarelli et al, ACS Appl. Mat. & Interf. (2022)

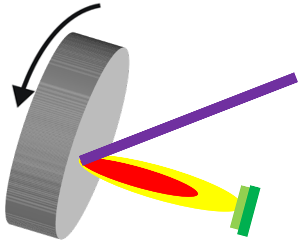

Low Temp PLD
A. Quetalto et al, SUST (2023)

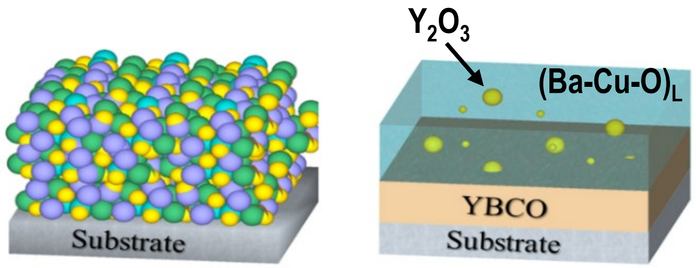

Nanocrystalline precursors

YBCO growth

- High performance (3 MA/cm^2 at 77K)
- High throughput
- Simple reactor
- Large area processing
- Low cost/performance method

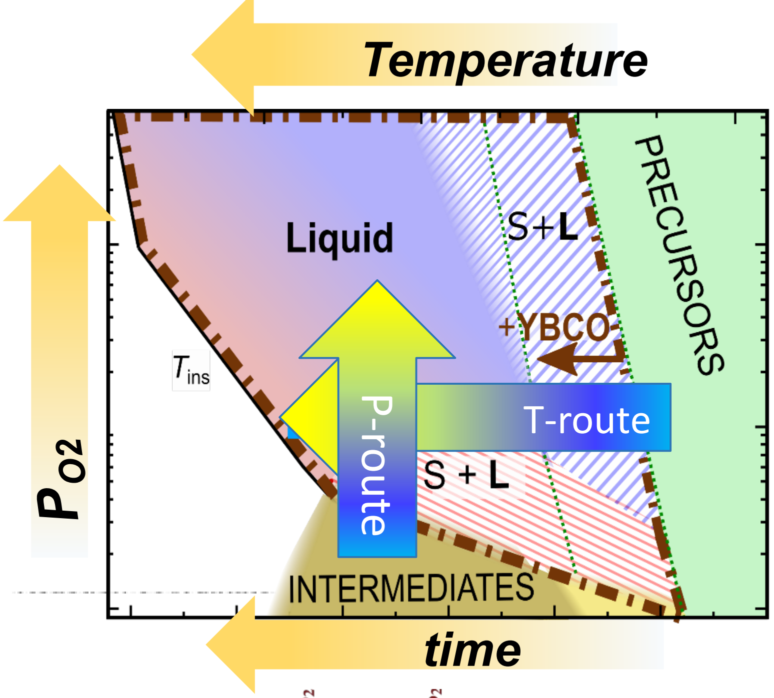

In-situ synchrotron XRD

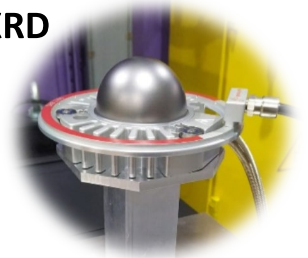

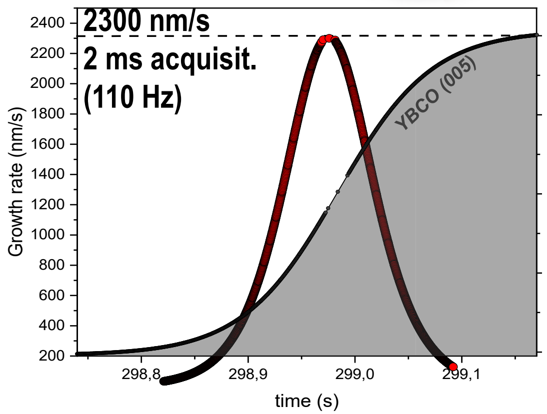

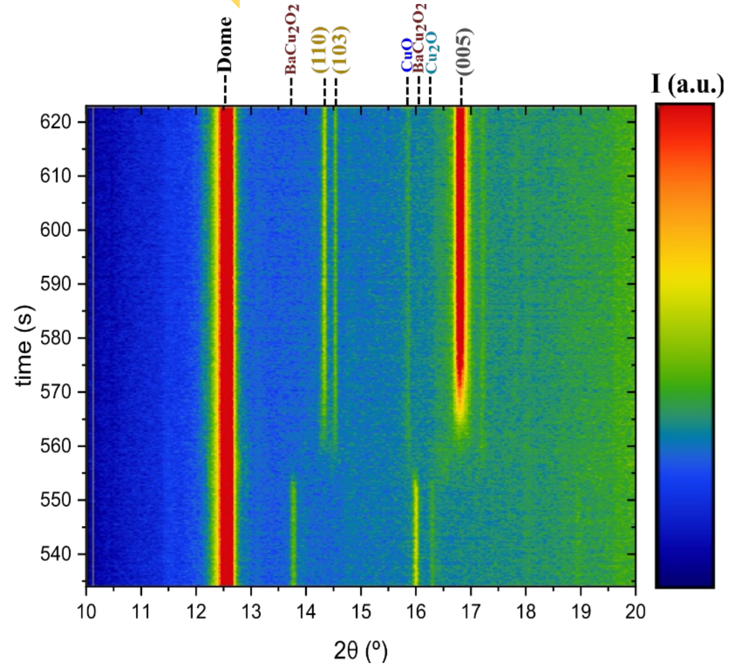

100 nm/s by **ultrafast-PLD** EuBCO/BHO (transient liquid growth at high T PLD)

Y. Wu, Materials & Design 224 (2022)

L. Soler et al., Nat Comm (2020), S. Rasi, et al, Advance Science (2022)

Reaching high Growth Rate: A path towards cost reduction

ICMAB INSTITUT DE CIÈNCIA DE MATERIALS DE BARCELONA EXCELENCIA SEVERO OCHOA

Figure of merit: $\frac{Cost}{Perfomance} = \frac{total\ cost\ per\ year}{G\ x\ L\ x\ W\ x\ (I_{c-w}/d)} = \frac{€}{kA\ x\ m}$

W= tape width
L= tape length
d=tape thickness

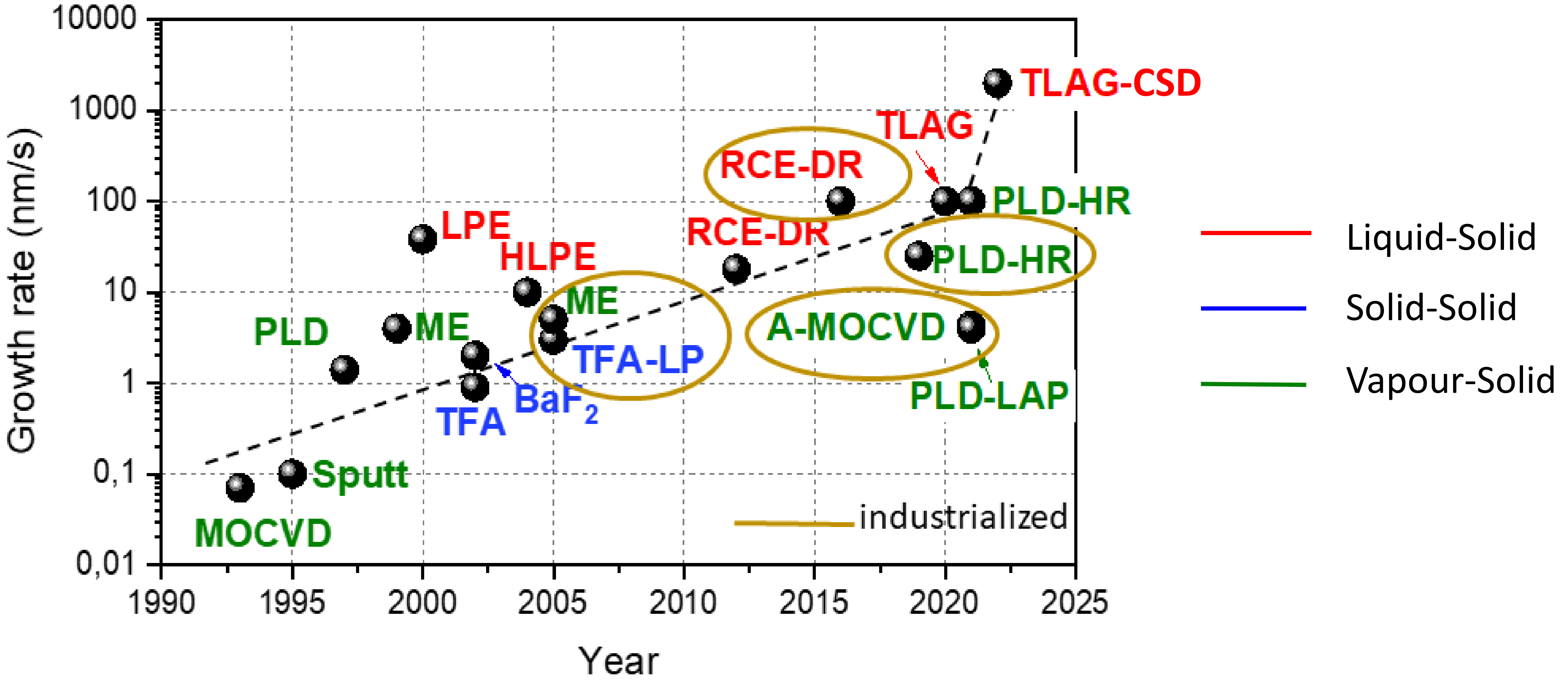

T. Puig, J. Gutiérrez, X. Obradors Nat Rev Phys (2023, doi.org/10.1038/s42254-023-00663-3);

The complex defect structure in nanocomposites

Relevant issues: size, dimensionality, orientation, concentration

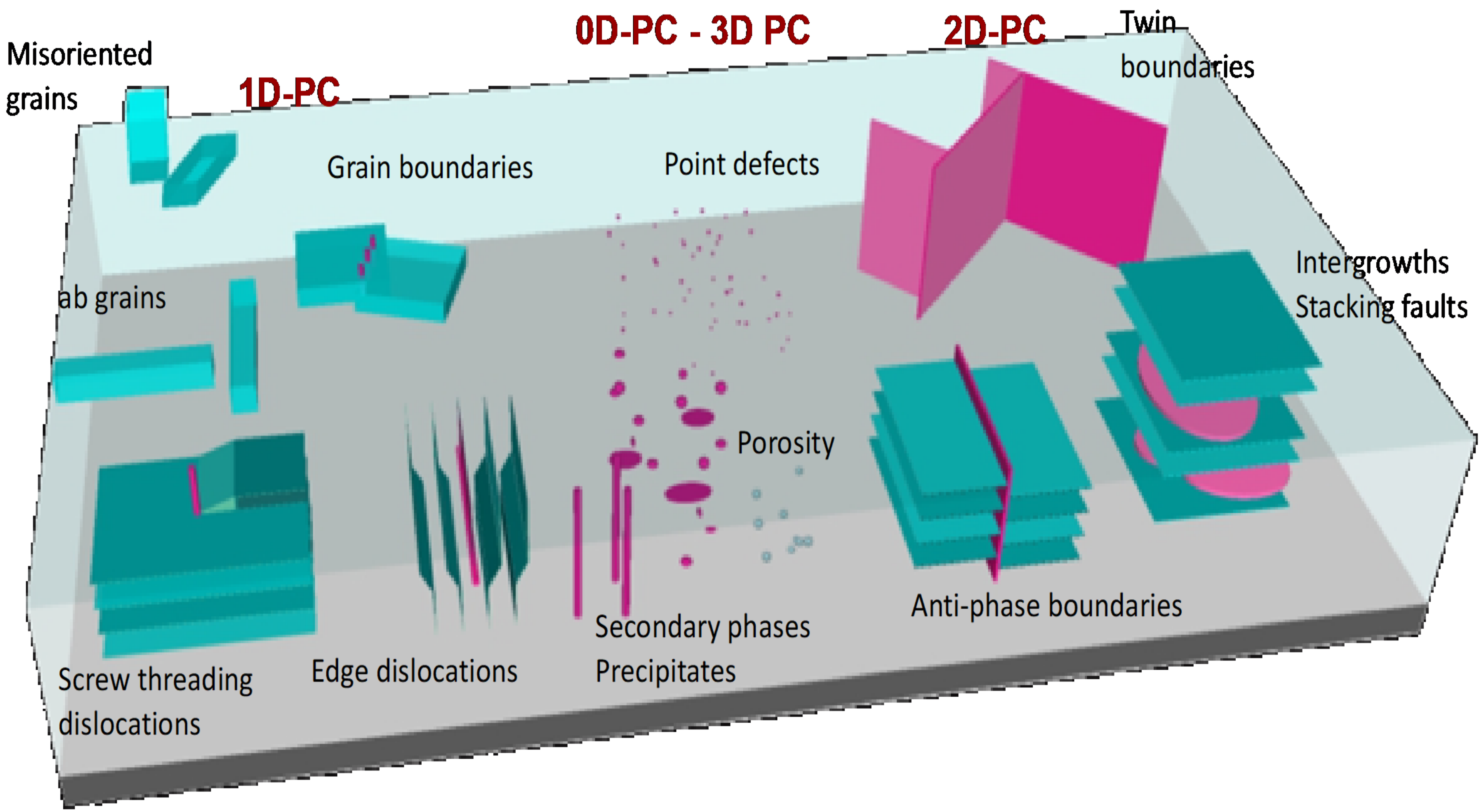

Different growth methods have modified nanostructures

The complex magnetic phase diagram of nanocomposites

Relevant issue: behaviour of defects as APCs can be classified as weak or strong and isotropic or anisotropic

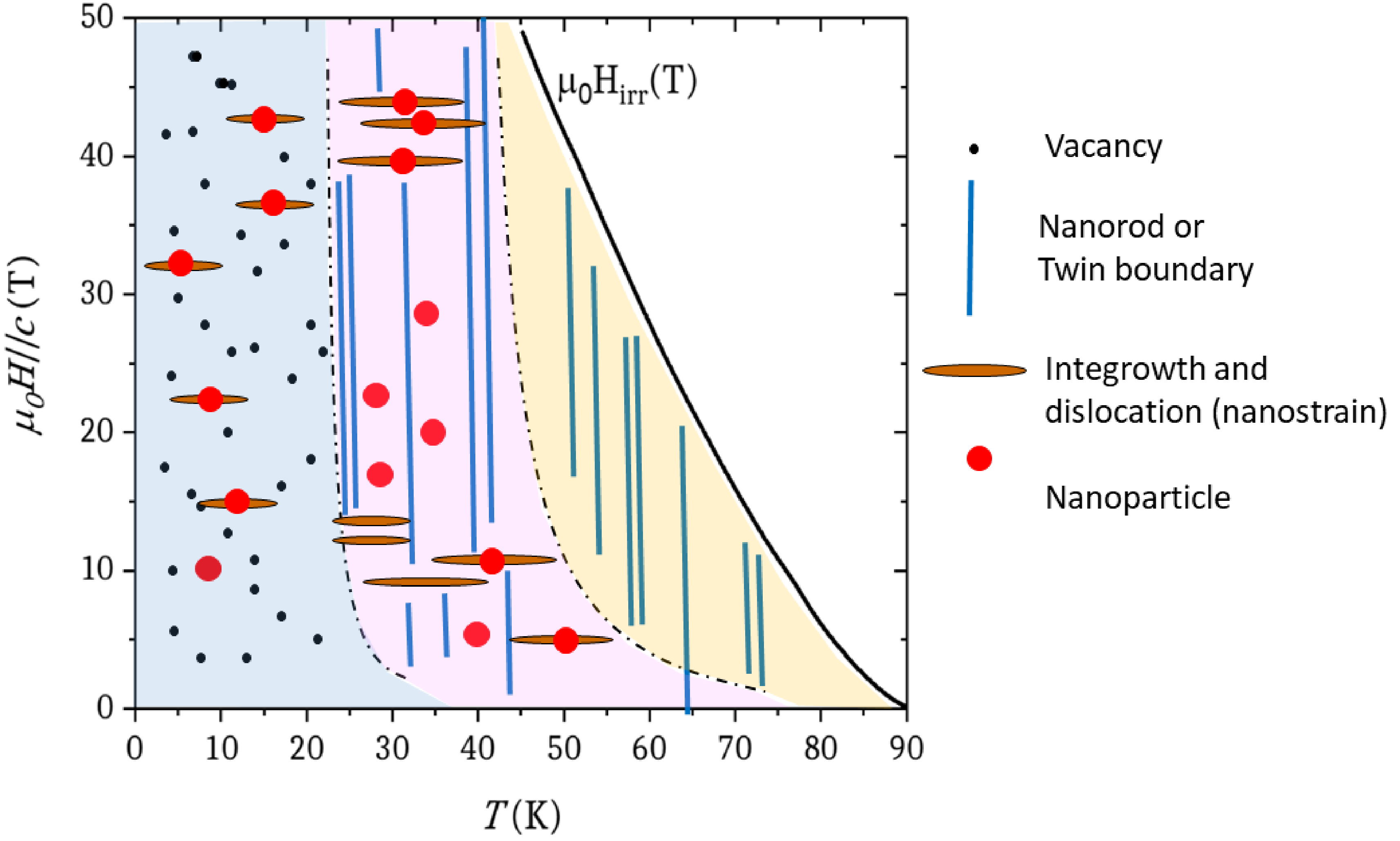

We need a simple route to classify defects behaviour in terms of vortex pinning centers to follow the differences and the evolution of CCs with different processing methodologies and now with irradiation !

Simultaneous deposition/growth: micro/nanostructure

BaZrO_3 nanocolumns

PLD

Vapour - solid growth: low growth rates (1 - 4 nm/s)

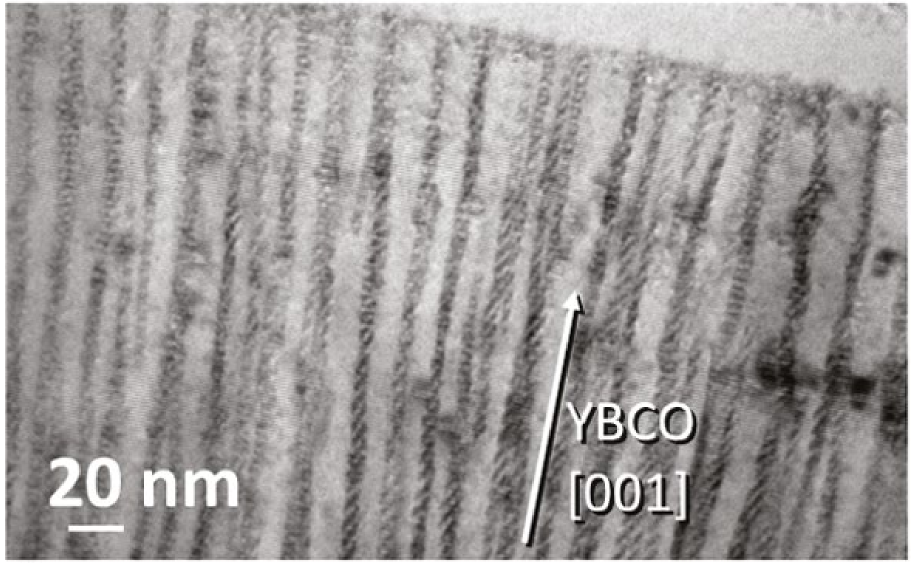

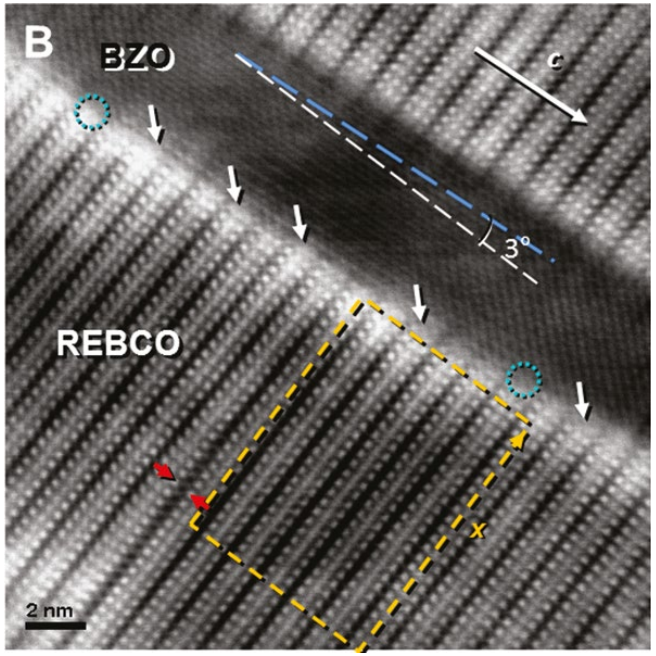

(Gd,Y)BCO / BZO nanorods
5-6 nm diameter, separation : 18 nm
Growth rate: 4 nm/s

A-MOCVD

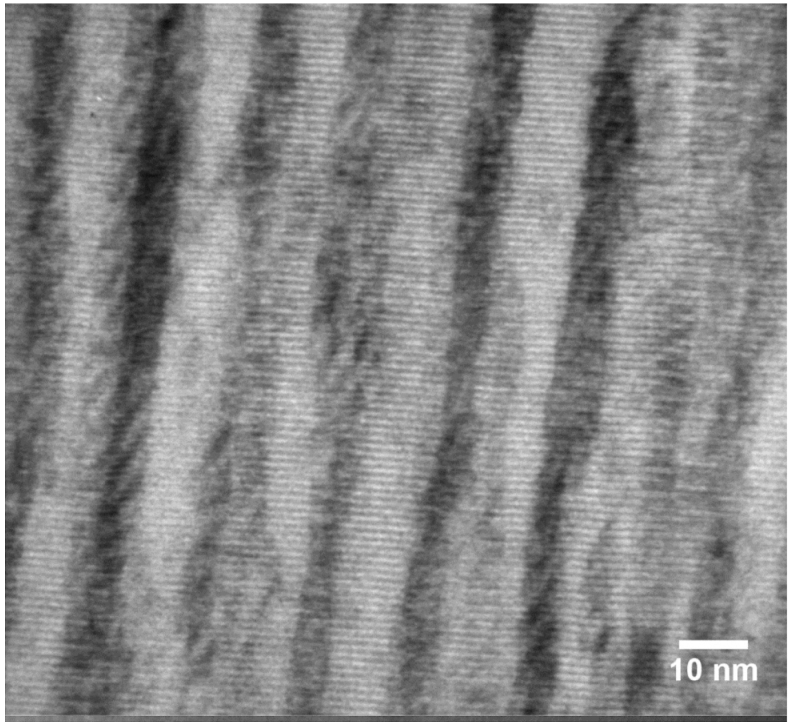

Strain field develop around the nanocolumns to reduce boundary energy inducing self-assembly
Oxygen vacancies and misfit dislocations at the interface

C. Cantoni et al , ACSNano (2011)

Nanorods (BZO) + nanoparticles (Y_2O_3): Maiorov et al. Nature Mat. 8 (2009)
Nanoparticles (Y_2O_3): Molodyk et al. Sci Reports (2021)

G. Majkic et al., SUST (2020)

Simultaneous growth films: micro/nanostructure

PLD-LAP (YBCO-BYTO)

Liquid assisted growth: fast growth rates (5 - 100 nm/s)

PLD-HR (EuBCO- BHO)

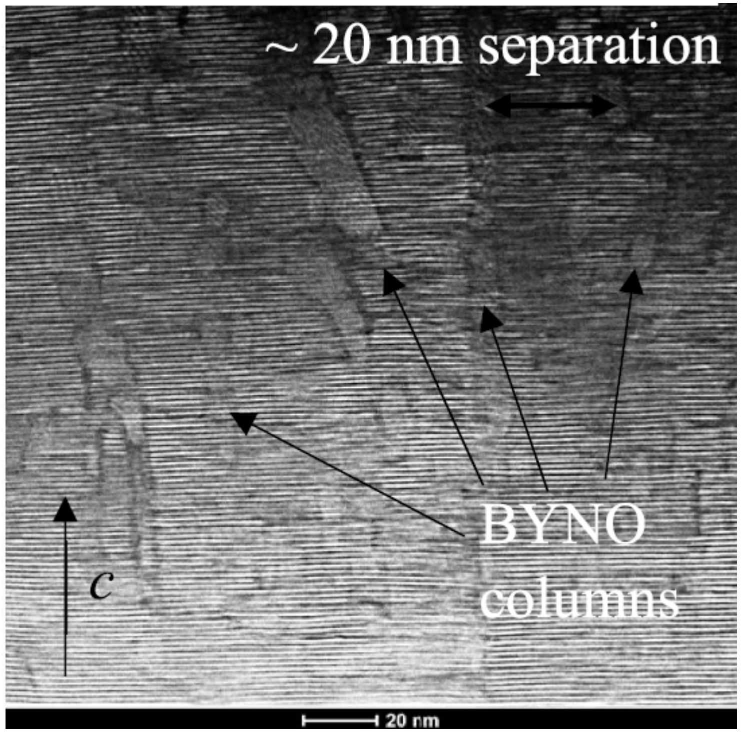

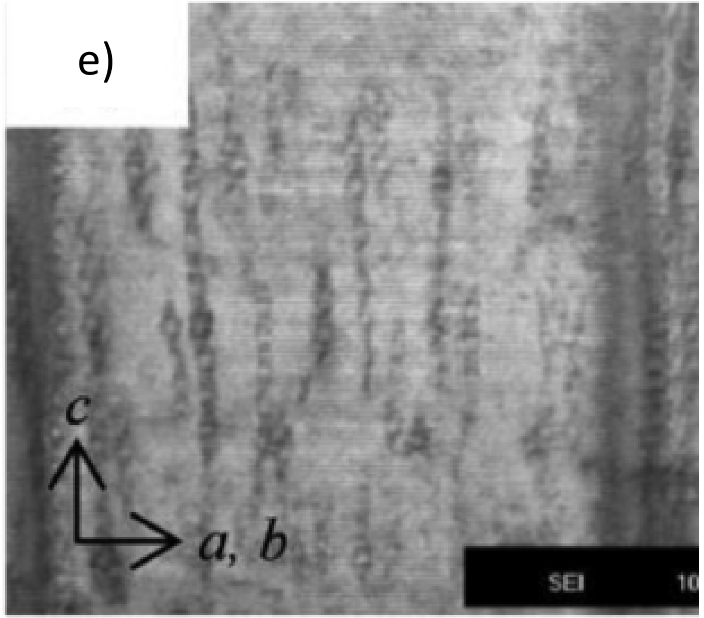

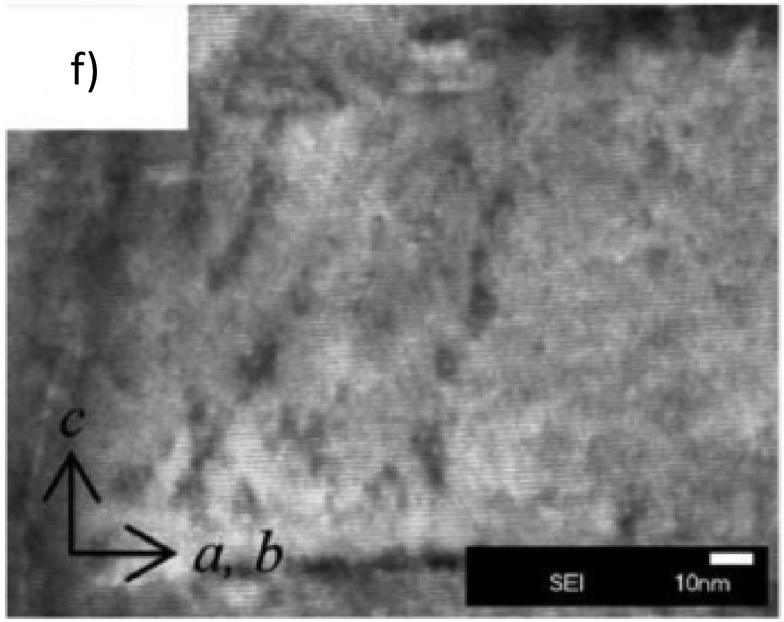

4 nm/s: BYTO nanorods misalignment

5 – 15 nm/s: discontinuous aligned BHO nanorods

20 – 30 nm/s: strongly segmented and misaligned BHO nanorods

J. Feighan et al., SUST (2021)

S. Fujita et al., IEEE Trans Appl Supercond. (2019)

Simultaneous growth films: micro/nanostructure

Liquid assisted growth: fast growth rates (20 - 100 nm/s)

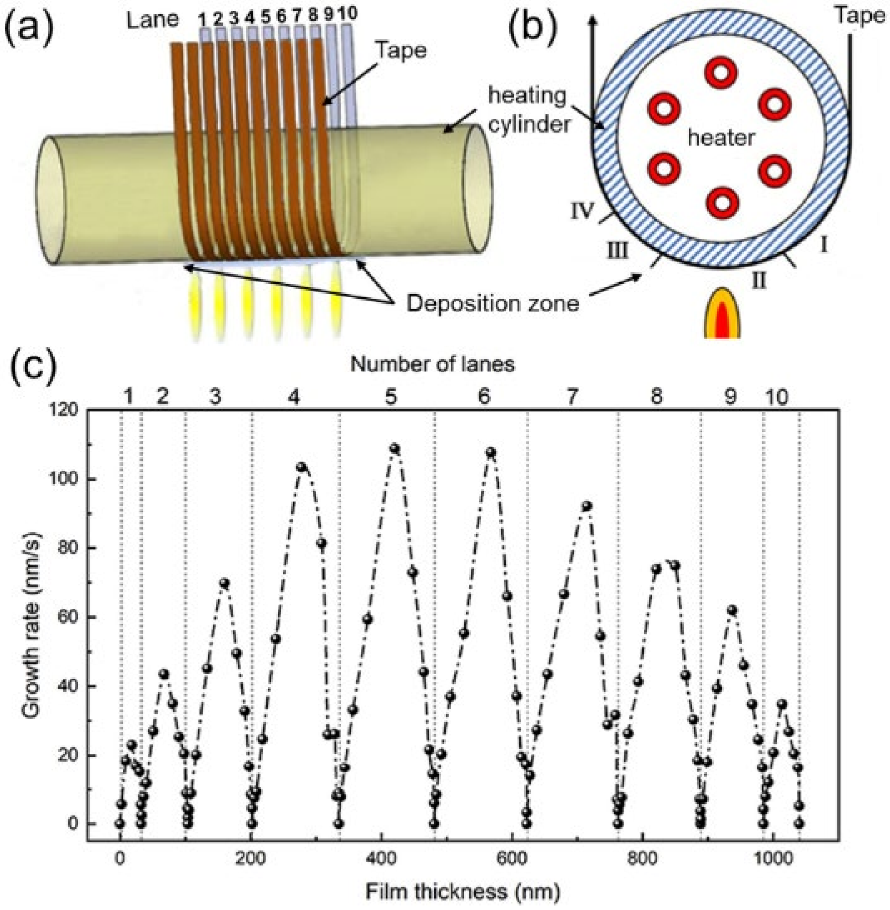

4 nm/s: BYTO nanorods misalignment

Y. Wu et al., Mat & Design (2022)
Shanghai Superconductor Technology

PLD-HR (EuBCO- BHO)

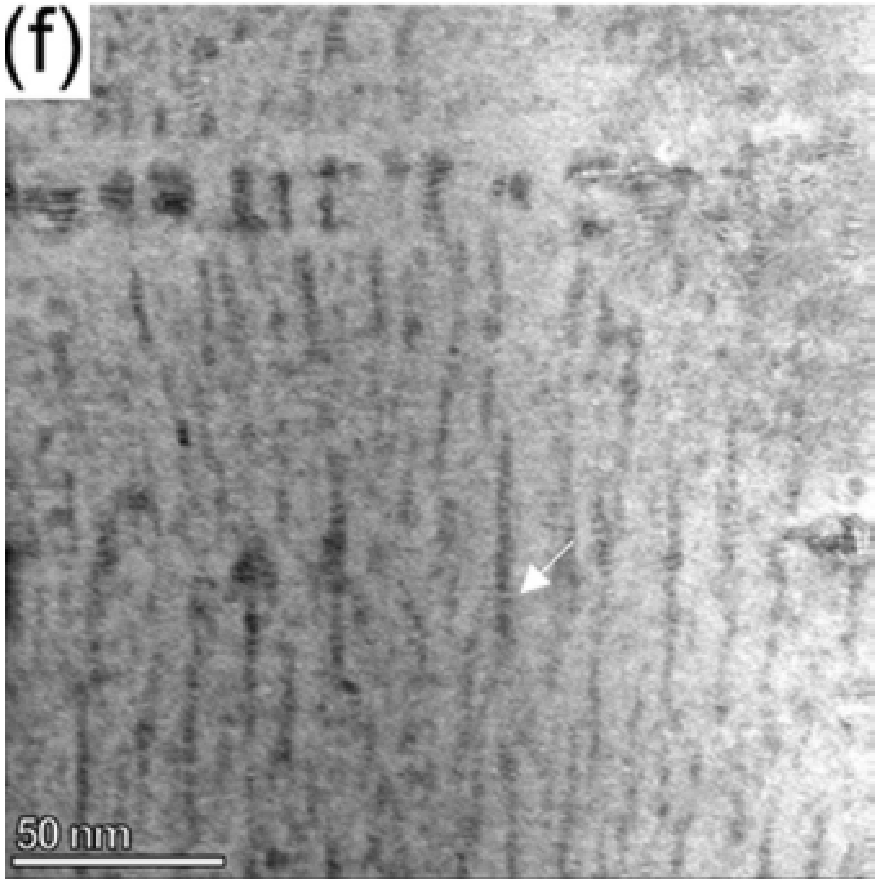

20 – 100 nm/s: strongly segmented and misaligned BHO nanorods

Simultaneous growth of Nanocomposites
Low versus high growth rate

Grown at 0.6 nm/s

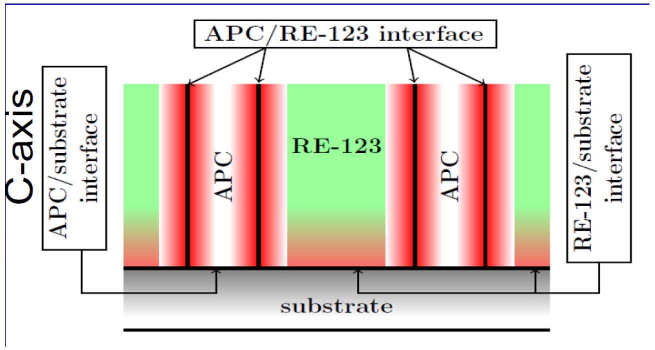

Elastic Strain energy model

Wu, et al, SUST 30 (2017)

High growth rates (10-50 nm/s)

Montecarlo simulations

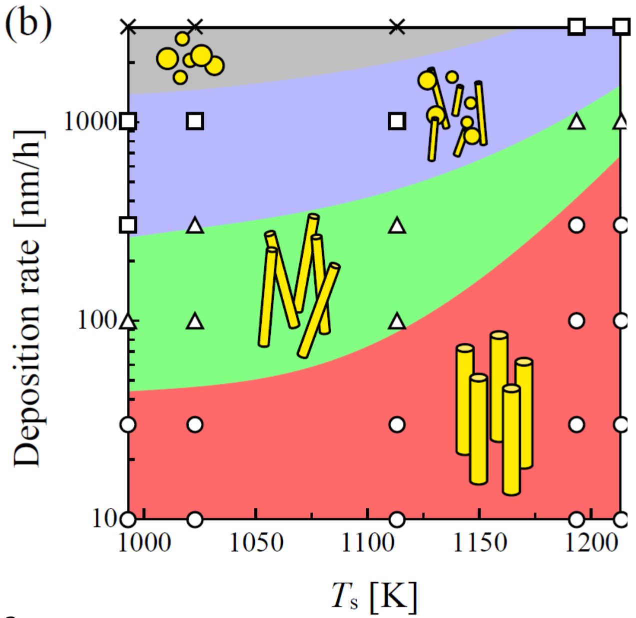

Y Ichino et al J.JAP 56 (2017)

EuBCO + $HfBaO_3$ nanorods

20-30 nm/s

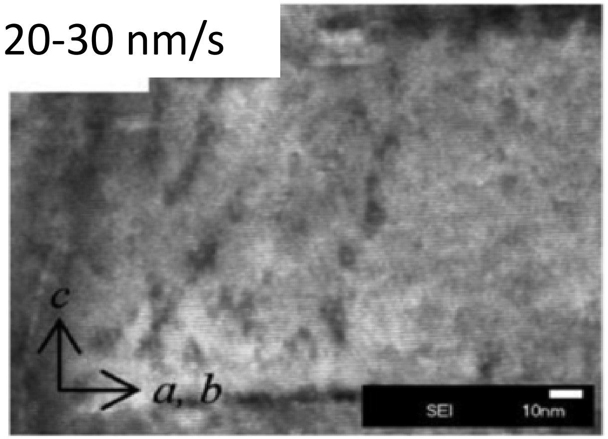

10-15 nm/s

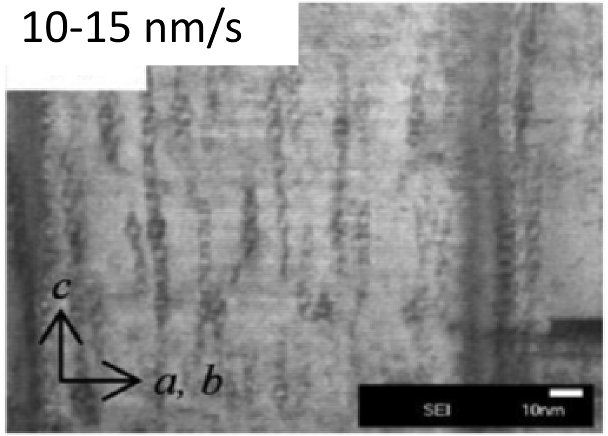

Fujita, S. et al. IEEE TAS 29 (2019)

Engineering landscape by design

LTG – PLD method

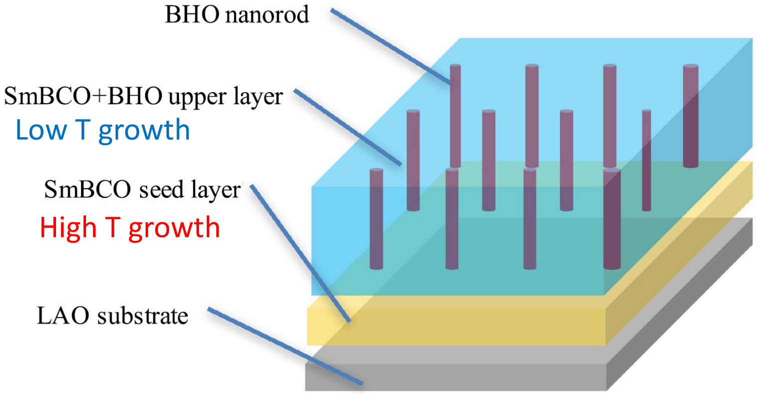

Y. Yoshida et al, SUST 30 (2017)

dynamic control of nanorod / YBCO interface

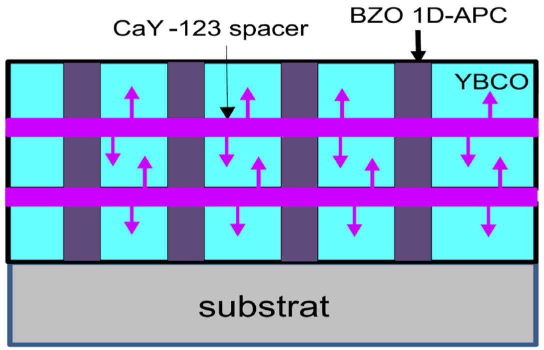

Wu, et al, SUST 35 (2022)

Sequential deposition and growth films (CSD, RCE-DR)

Use of complex solutions for spontaneous segregation of nanoparticles (TFA) ($BaZrO_3$, $BaHfO_3$, Ba_2YTaO_6, $BaCeO_3$)

- J. Gutierrez et al, Nat Mat (2007);
- A. Llordés et al, Nat Mat (2012)

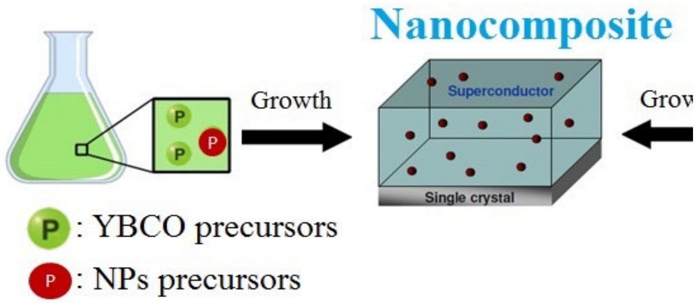

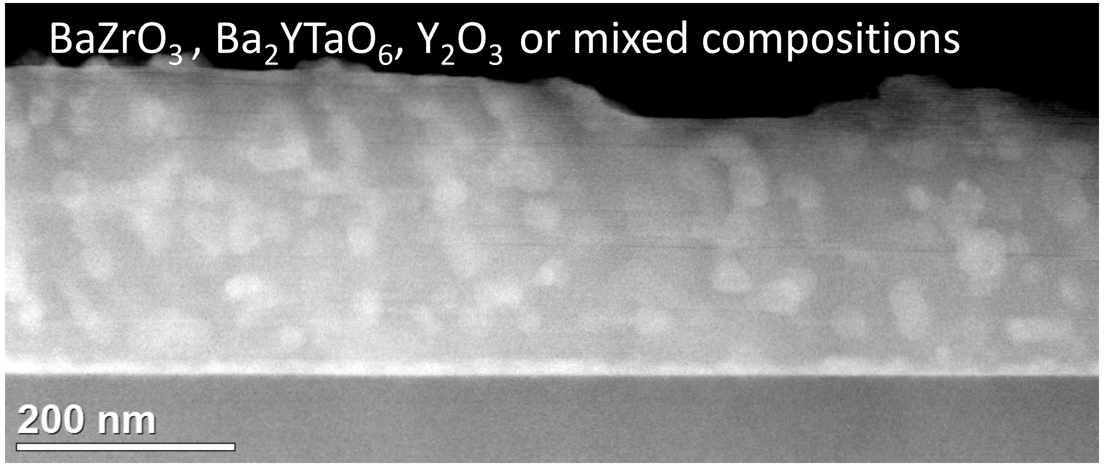

Not suitable for TLAG

pn-Nanocomposites: Colloidal solutions with preformed nanoparticles (N. Chamorro, RSC Adv. (2020)

Suitable for TFA and TLAG

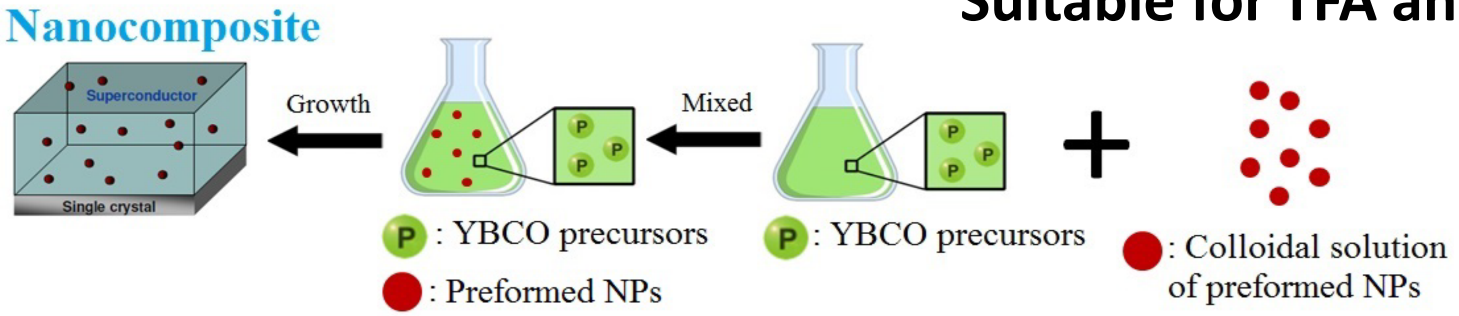

- Spinel (MFe_2O_4)
- Fluorite (CeO_2, ZrO_2)
- Perovskite $BaMO_3$ (M= Zr, Hf)
- Bronze $Ba(Ta,Nb)_2O_6$

Need to stabilize np in the alcoholic and ionic environment of YBCO precursor solution at high concentrations

- P. Cayado et al, SUST (2015)
- X. Obradors et al, SUST (2018)
- D. Garcia et al., to be published

Nanoparticles for multifunctional colloidal solutions

ICMAB
INSTITUT DE CIÈNCIA DE MATERIALS DE BARCELONA
EXCELENCIA SEVERO OCHOA

Requeriments

NP solution

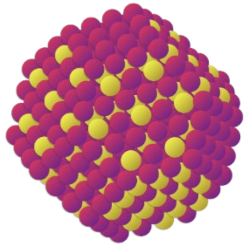

Small-size < 10 nm

Non-aggregation
in alcohol solution

High concentrations in
alcohol solution
(≥ 100 mM)

Stabilization in YBCO precursor solution

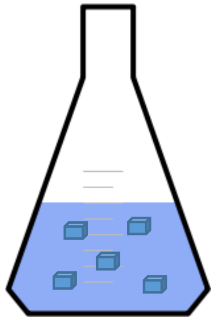

NPs compatible and stable
in YBCO precursor solution
-non- aggregation
-no precipitation

Compatibility with CSD-TLAG process

NP composition non-reactive
with YBCO

High-thermal stability of
NP composition

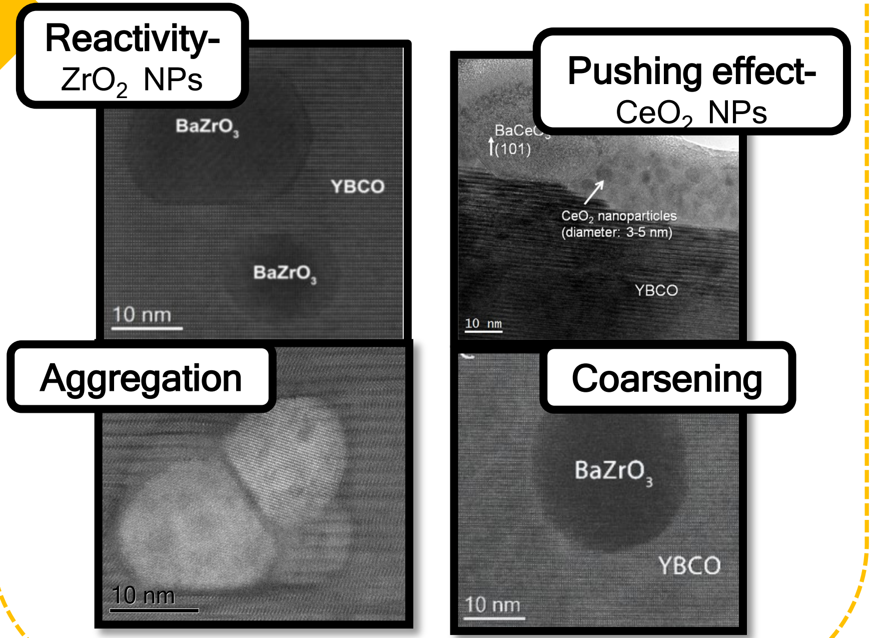

$Ba(Zr,Hf)O_3$
$Ba(Ta,Nb)_2O_6$

Multifunctional colloidal ink
(Patent EP22382741)

N. Chamorro et al, RSC Adv. (2020)

$BaMO_3$ (M= Zr and Hf) Nanoparticles

EXCELENCIA SEVERO OCHOA
ICMAB
INSTITUT DE CIÈNCIA DE MATERIALS DE BARCELONA

$BaZrO_3$ NC

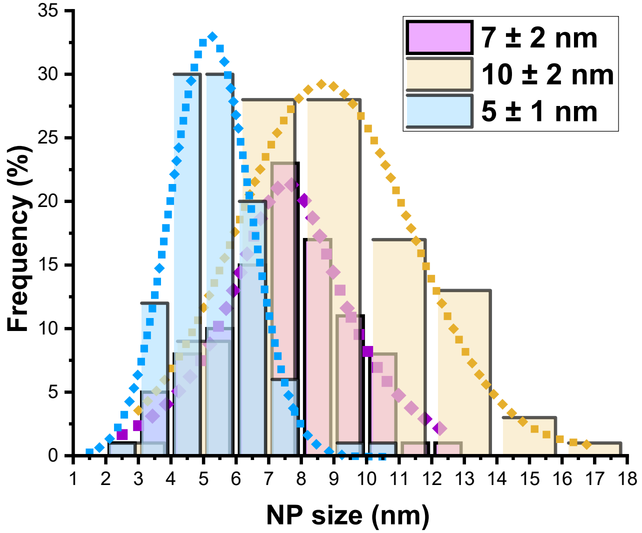

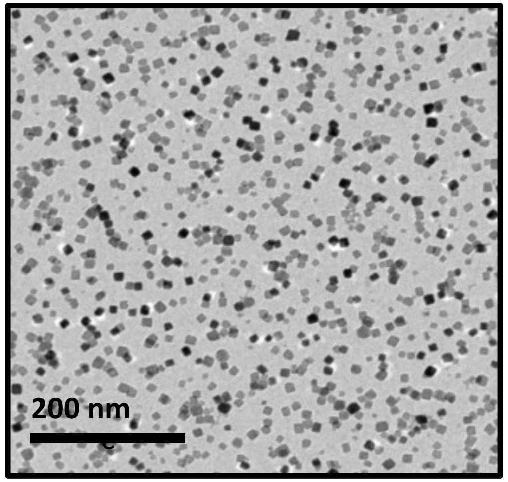

$BaHfO_3$ NC

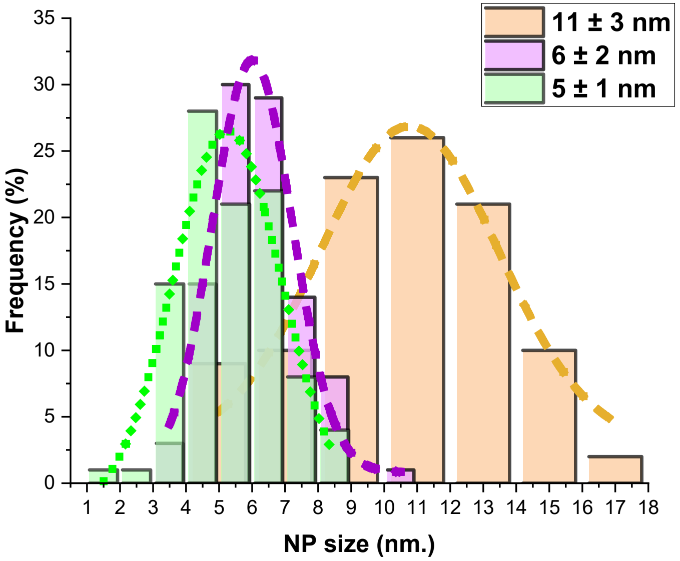

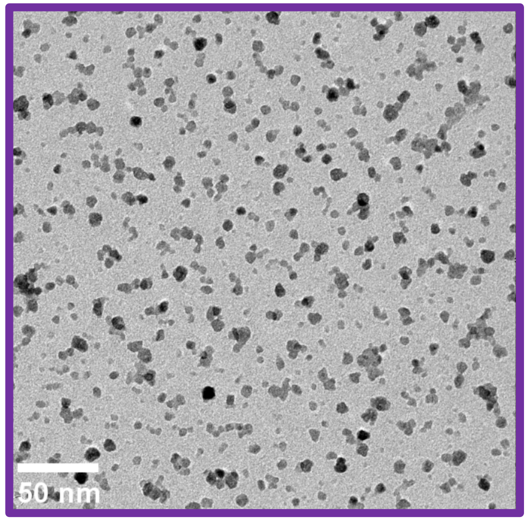

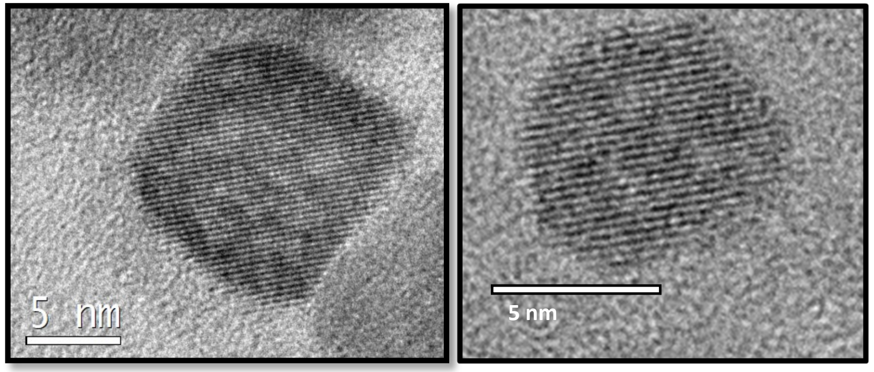

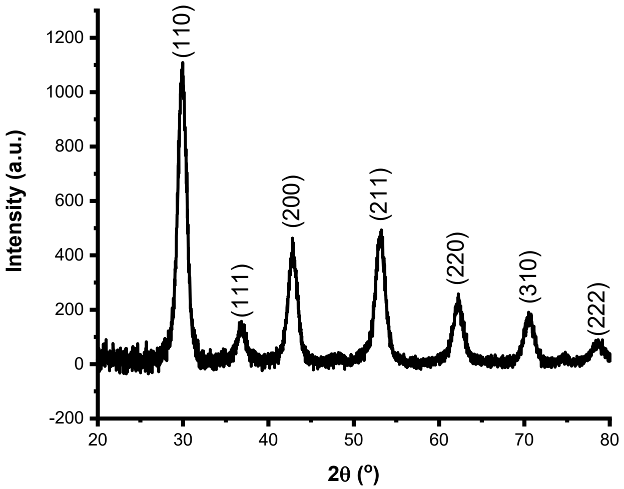

cubic phase

✓ Stable solutions (size/surface stability) for months

✓ Tuneable NP size from 4-20 nm

N. Chamorro et al, RSC Adv. (2020)

Nanoparticles induce stacking faults at the incoherent interface

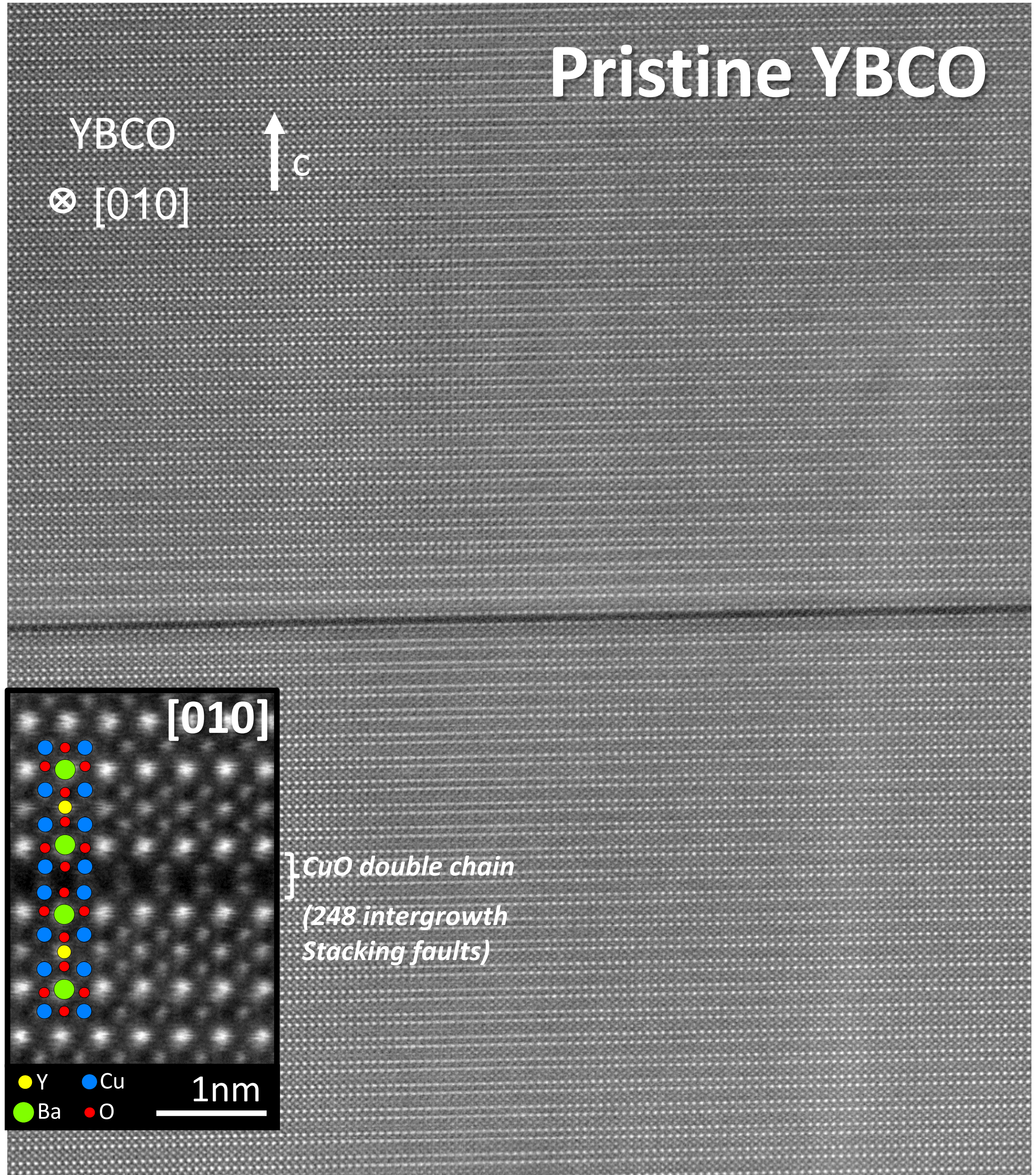

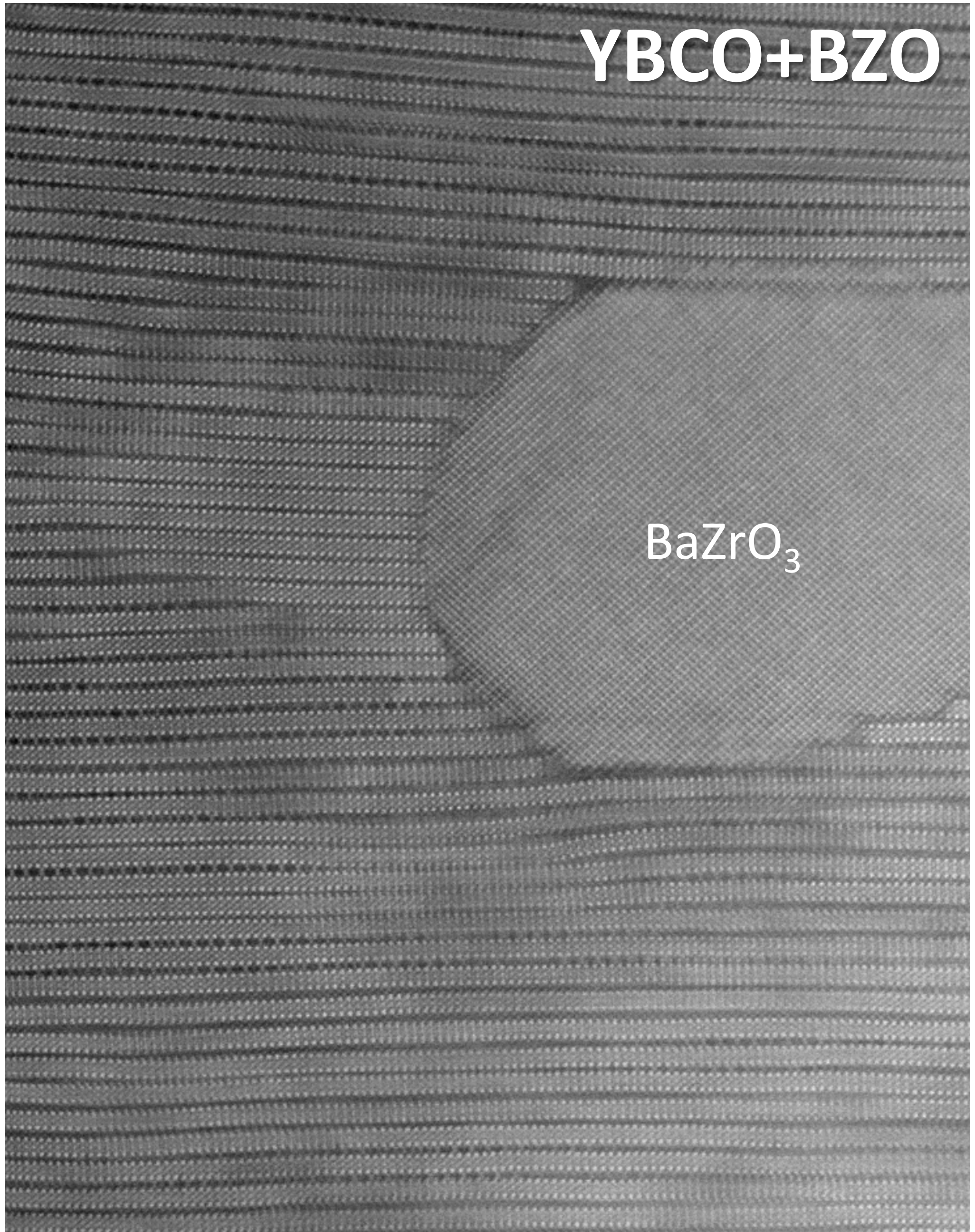

Incoherent YBCO-$BaZrO_3$ interfaces give rise to high density of Y248 intergrowths and associated nanostrain

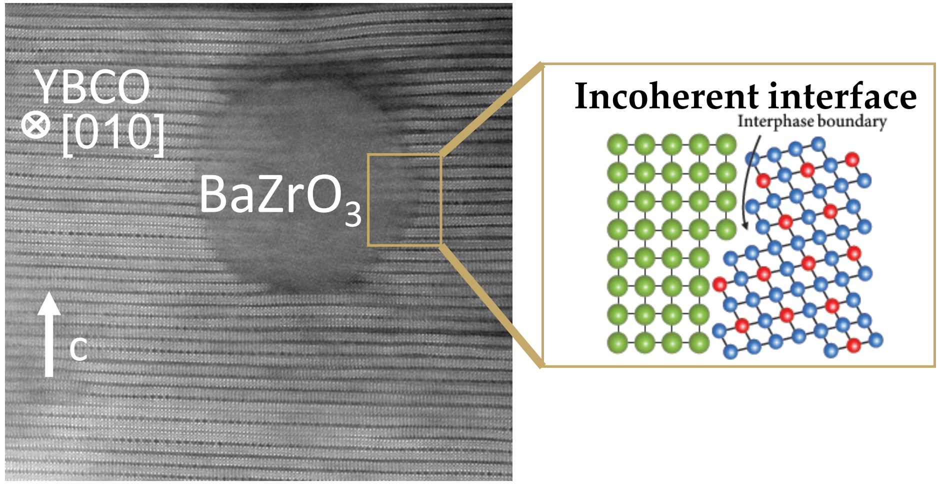

Incoherent interface is associated to the radom orientation of the nanoparticles

Strong strain effects are generated at the partial dislocations

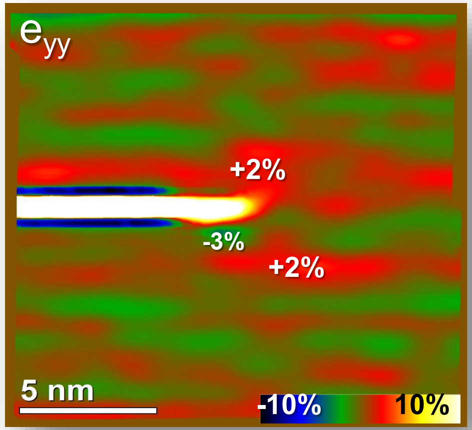

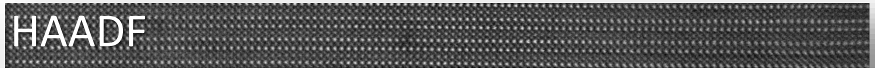

TFA Nanocomposites

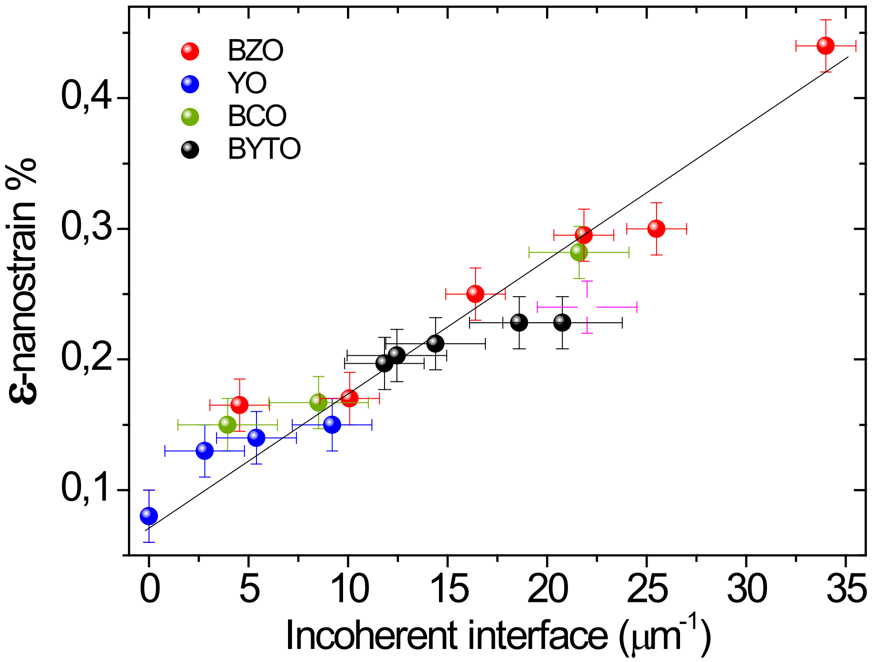

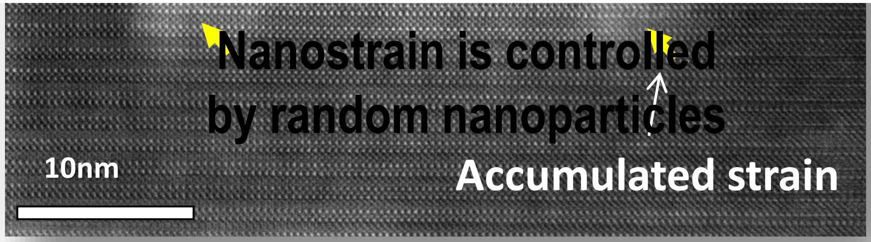

A. Llordés, et al. Nat. Mater , 11, 329 (2012), J. Gutierrez et al, Nat. Mater. 6, 367 (2007)

Partial dislocations surrounding SFs: source of isotropic nanostrain

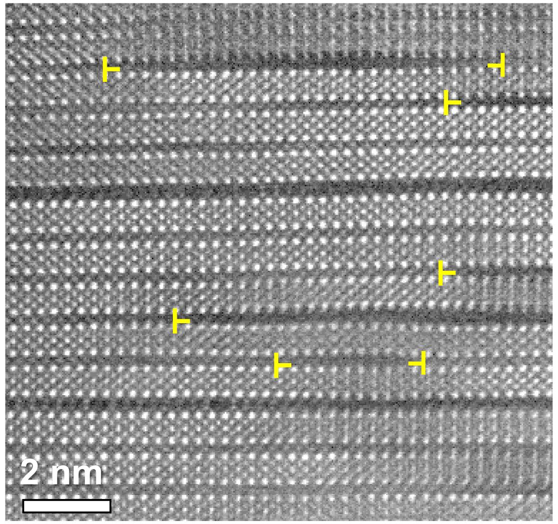

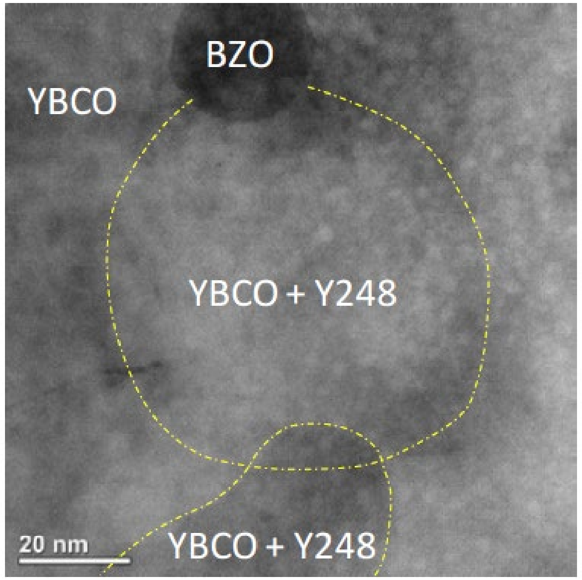

Plan view TEM

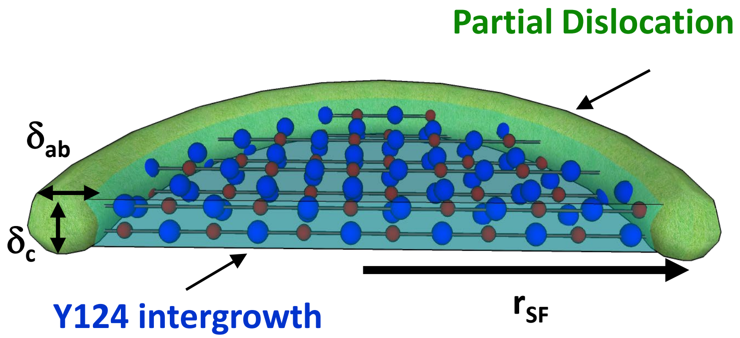

(Dislocation volume density from STEM images)

$$\rho_{dislocation} = \frac{\pi\delta_c\delta_{ab}}{\Delta x\Delta y\langle r_{SF}\rangle}\left(n_{SF}\delta_{ab} + 2\sum_{i=1}^{n_{SF}} r_{SF_i}\right)$$

Nanostrain can be easily measured by XRD and it controls the concentration of dislocations (TEM analysis) and nanometric disorder.

Vortex pinning is closely correlated to nanostrain

$\varepsilon = \Delta d/d$

d-spacing fluctuations

↓

defects

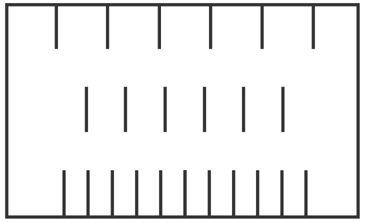

Non-uniform strain (nanostrain)

$\delta_i \sim 0.8$ nm

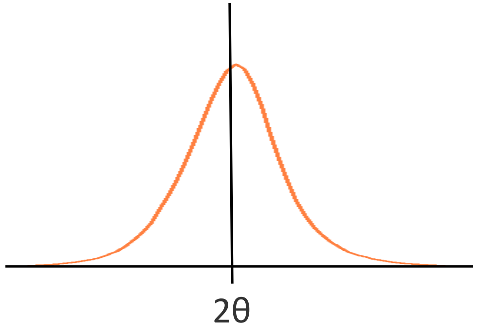

Williamson-Hall plot

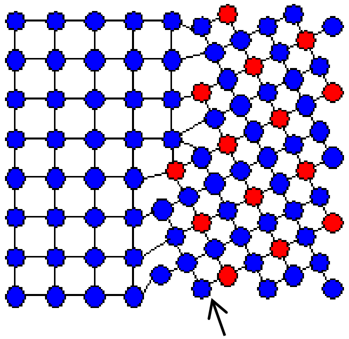

incoherent interface

Z. Li et al, Sci Rep. (2019)

Sequential deposition and growth films: micro/nanostructure

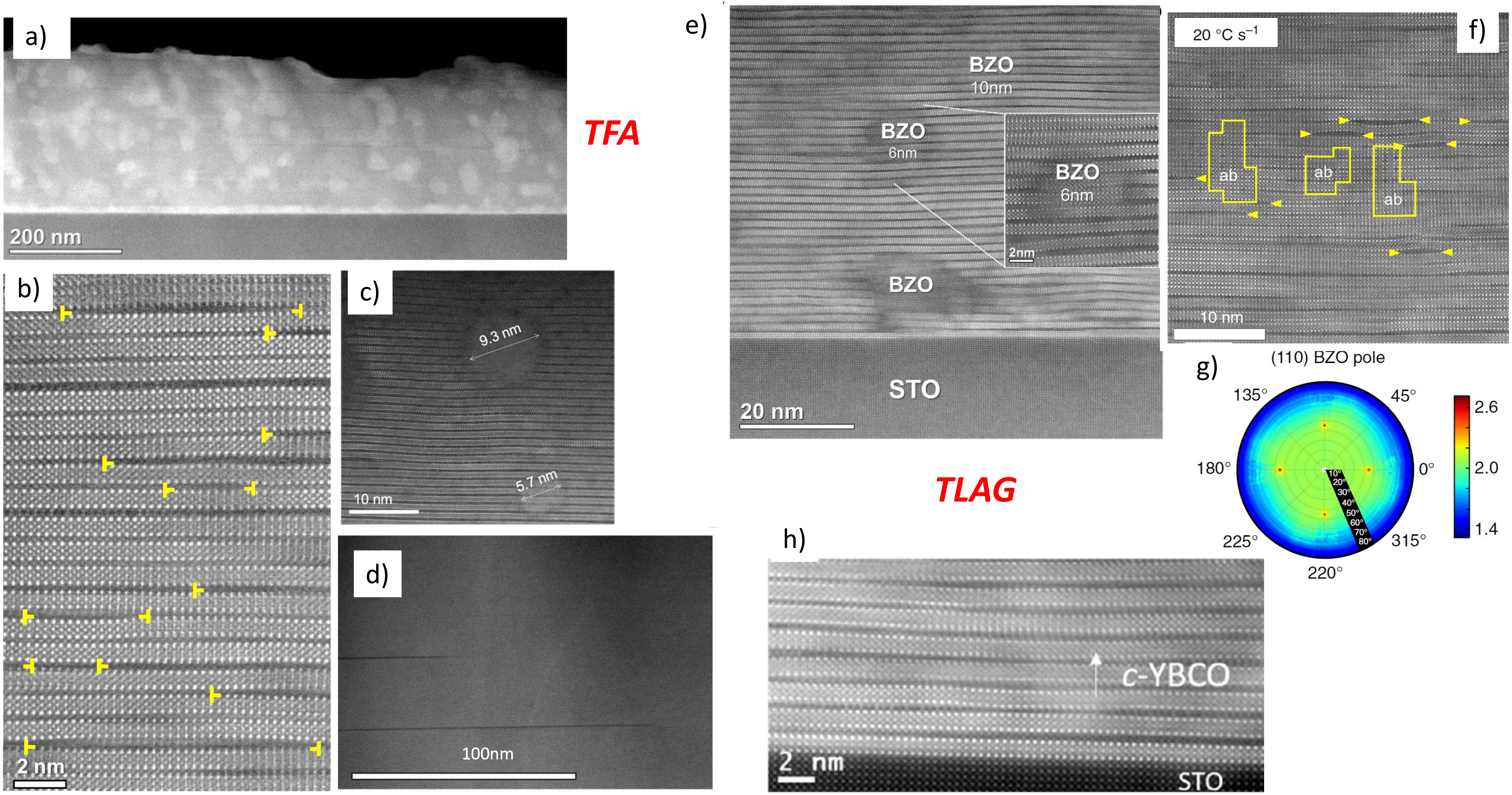

Weak pinning contribution: cation-oxygen vacancy clusters

Atomic scale defects (<1 nm) demonstrated

Cu – O vacancies within Y248 intergrowth → weak pinning ??

Avoids the Stoichiometry Catastrophe

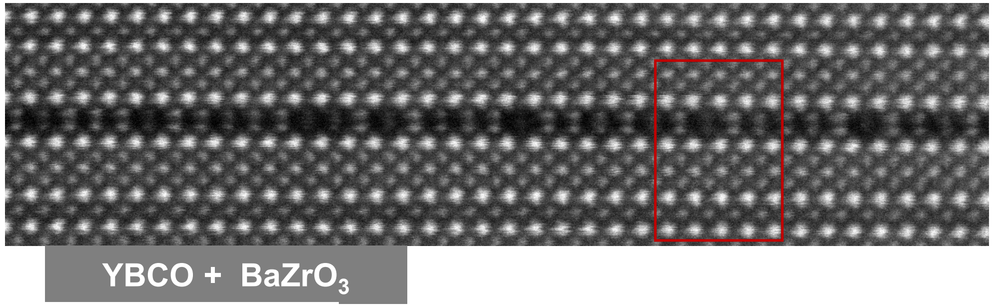

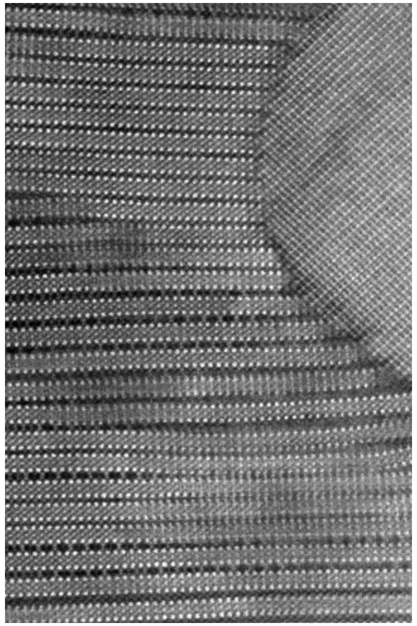

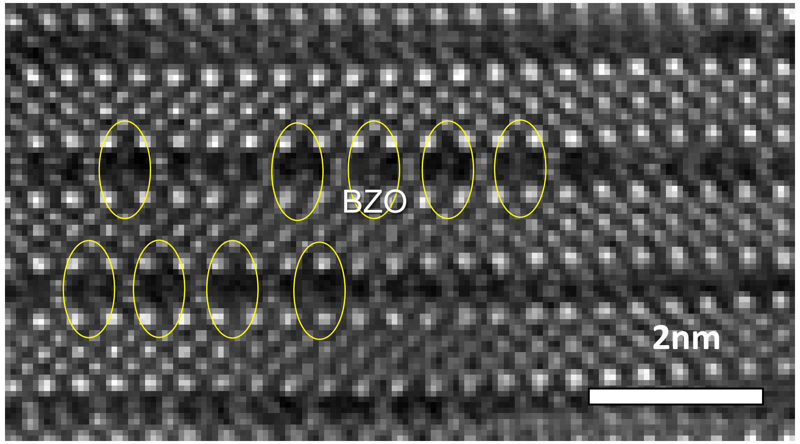

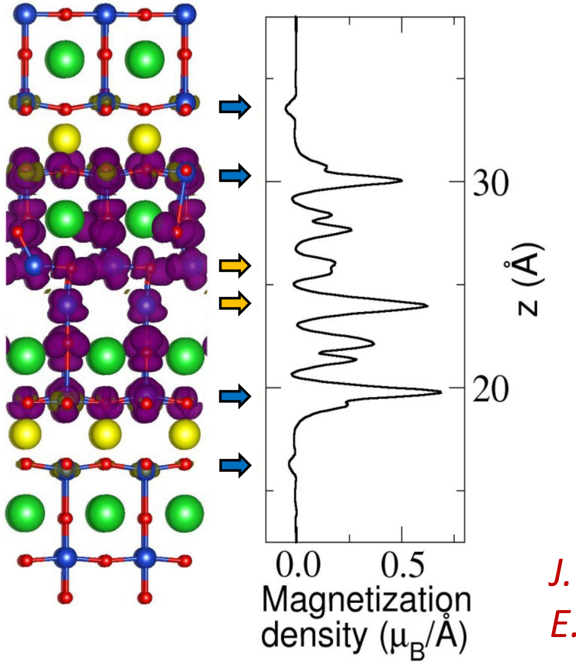

Cluster with ferromagnetism confirmed by XMCD synchroton radiation

Faulted Y248

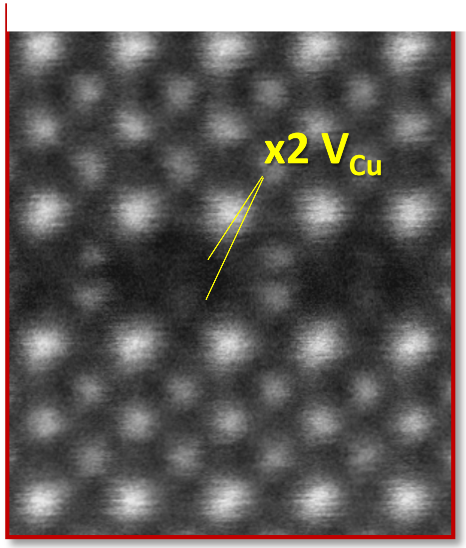

DFT calculations

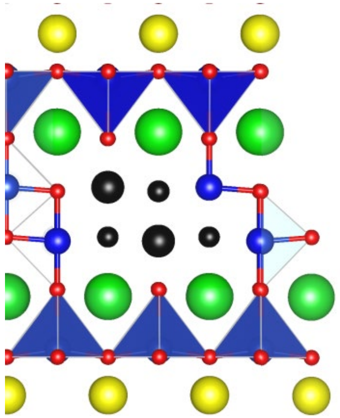

$2\ V_{Cu} + 3\ V_O^-$

E/Cu=1.1 eV

J. Gázquez et al, Adv. Science 3, 1500295 (2016)

E. Bartolomé et al., ACS Appl. Nano Mater. (2020)

TFA-BHO pn-nanocomposites by Flash Heating

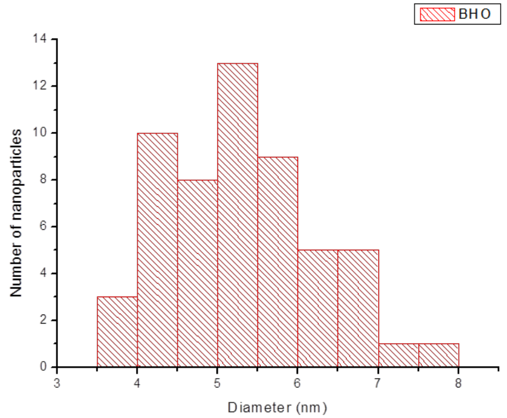

Distribution of initial NP: 4-6 nm

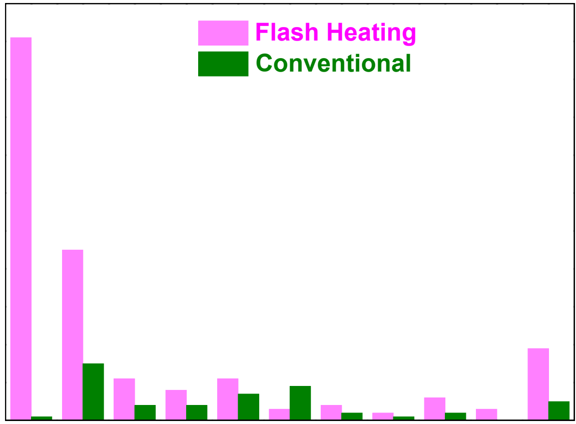

Flash heating (20 ºC/s): 20%M BHO (5 nm)

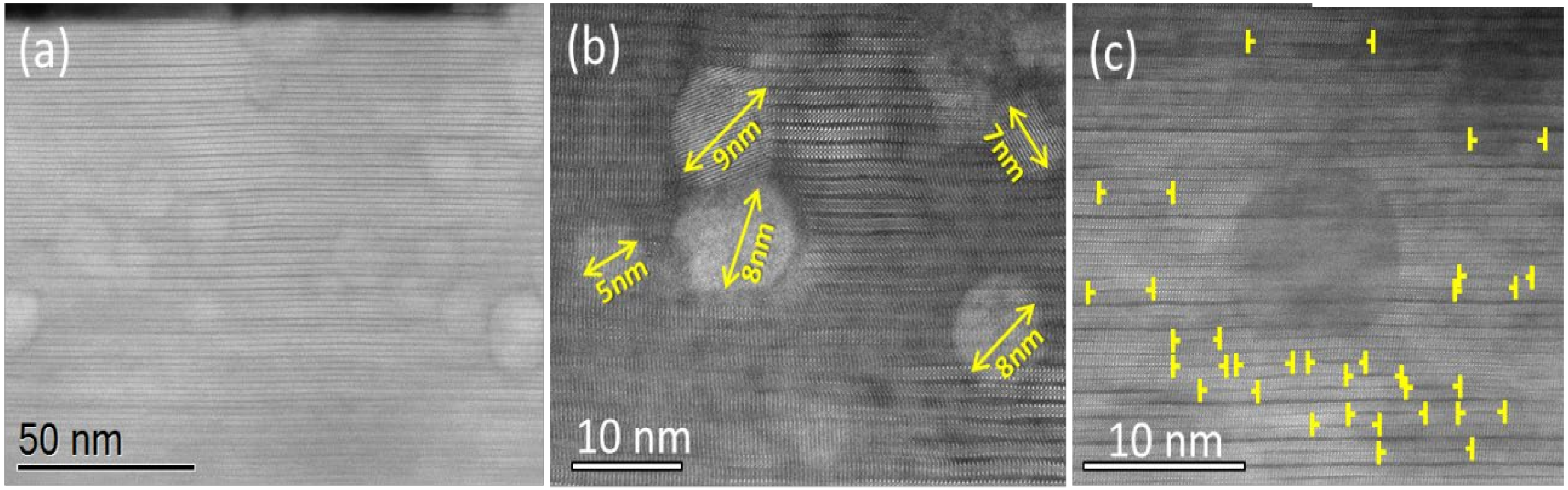

$n_{np} \approx 40 \times 10^{22}\ m^{-3}$ (x2,5) (≈ 8 % vol)
NPs random fraction: 94%

Short SFs are promoted ! (20 – 30 nm)
Vol density partial dislocation: ≈ 2.3 %vol

- Flash Heating strongly avoids NP coarsening
- Higher concentration of short SFs: higher density of partial dislocations
- NP size very close to the optimal size for vortex pinning (5-8 nm)

Z. Li et al, Sci Rep. (2019)
J Mat Chem C (2019)

UltraThin Once Coating (UTOC): a route to small NPs

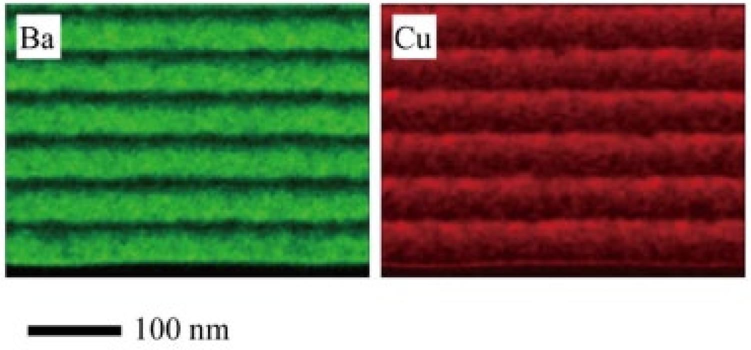

Multideposition with ultrathin repetition thickness (30 nm): CuO layers at the interfaces!

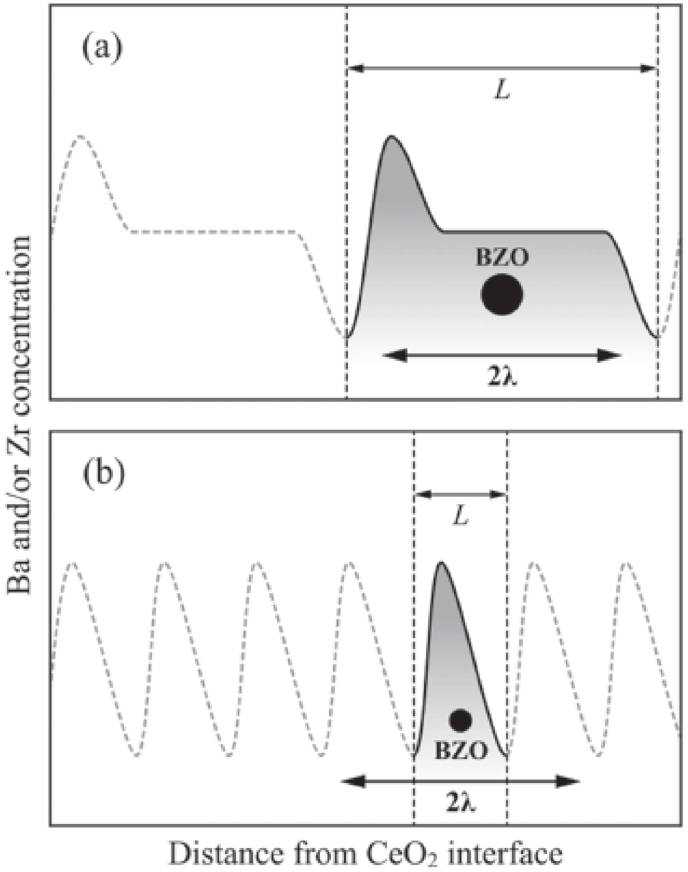

BZO and BHO nanoparticles are confined due to CuO barriers at the interface: coarsening is limited

(Y,Gd)$Ba_{1.5}Cu_3O_x$

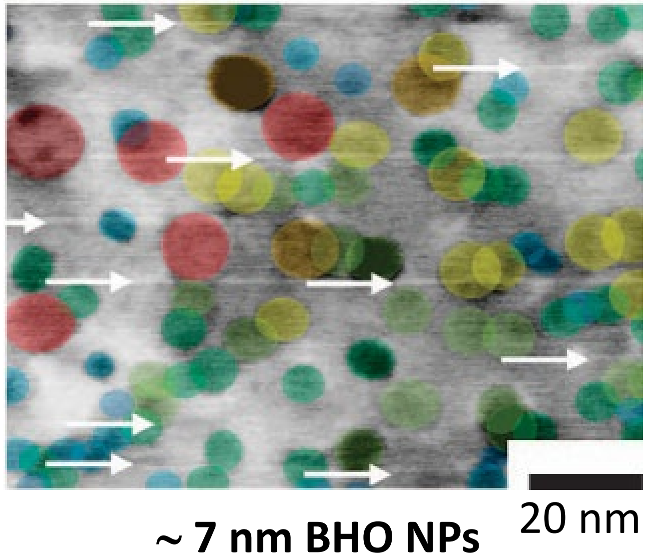

~ 7 nm BHO NPs

Very high concentration of small and dispersed NPs

Volume similar to the optimal in simultaneous growth approach

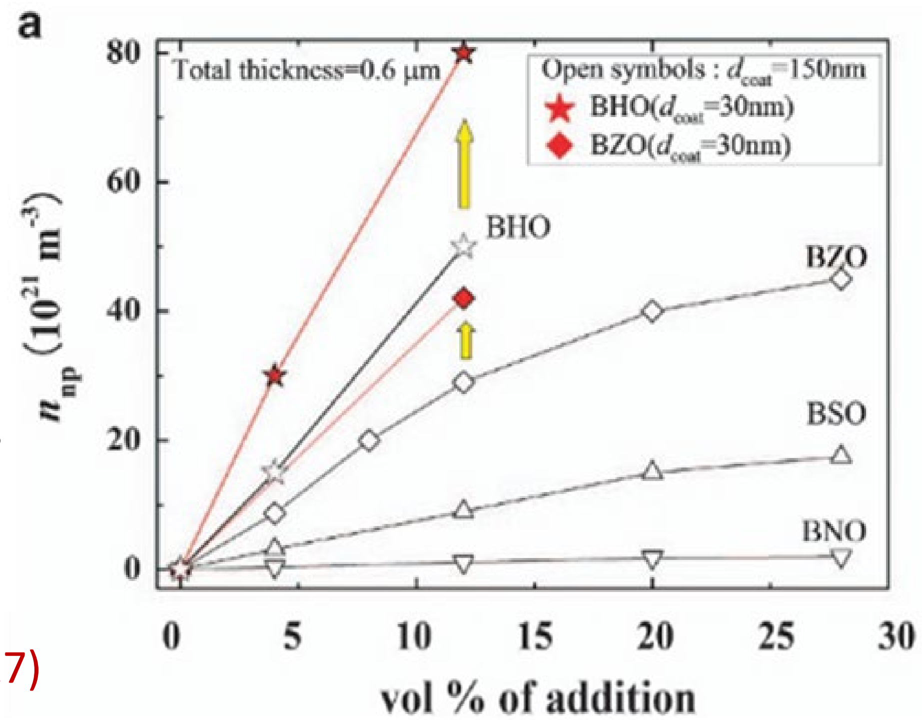

T. Izumi et al., SUST (2018)

M. Miura et al., NPG Asia Materials (2017)

Magnetic field dependence of $J_c(B,T)$: single vortex to collective pinning

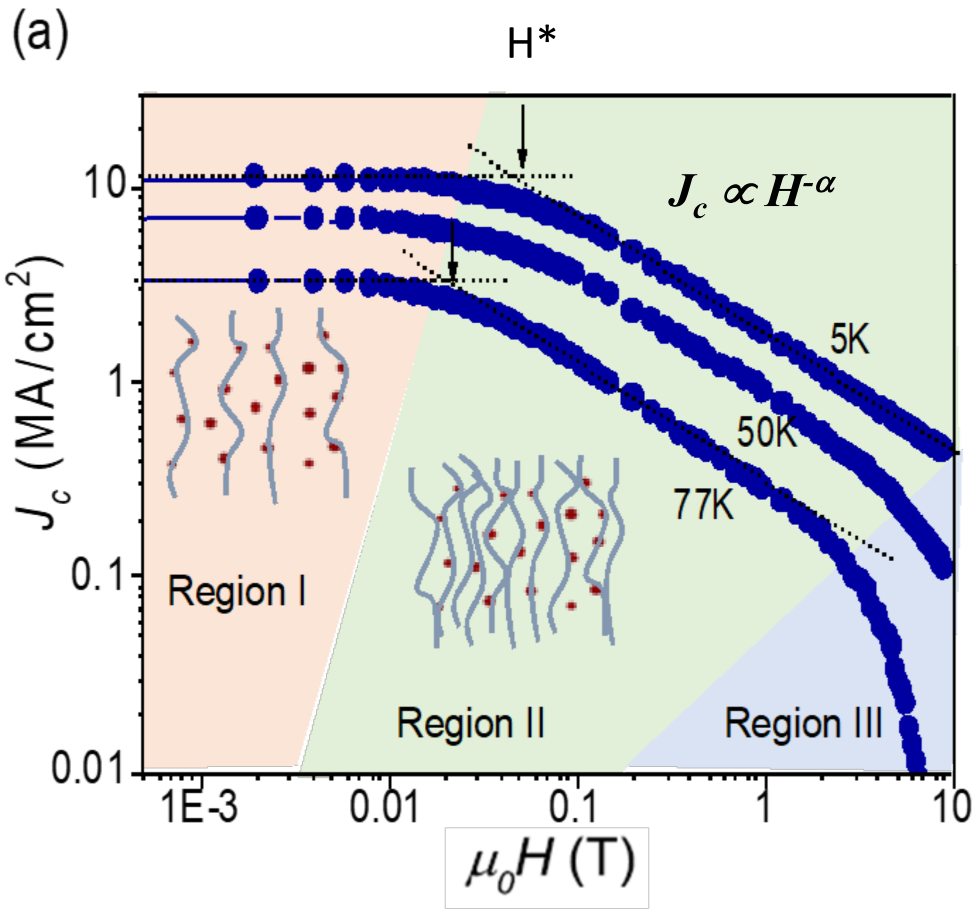

Region I: single vortex pinning (H*)
Region II: collective vortex pinning
Region III: thermal activation effects very relevant (close to H_{irr}(T))

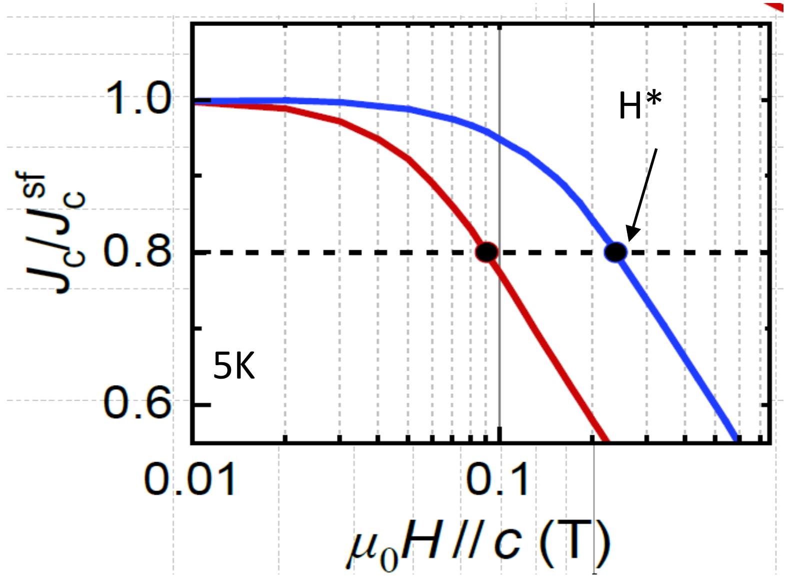

H*: single vortex regime (*measure of the density of pinning centers)*

Accomodation magnetic field H*(T): very useful parameter to monitor efficiency and concentration of APCs

A decrease of α values when the nanoparticle concentration is increased (enhanced vortex pinning)

Vortex pinning consequences at high growth rate: PLD-HR

"Tsunagu" Technology Fujikura

EuBCO + $HfBaO_3$ nanorods

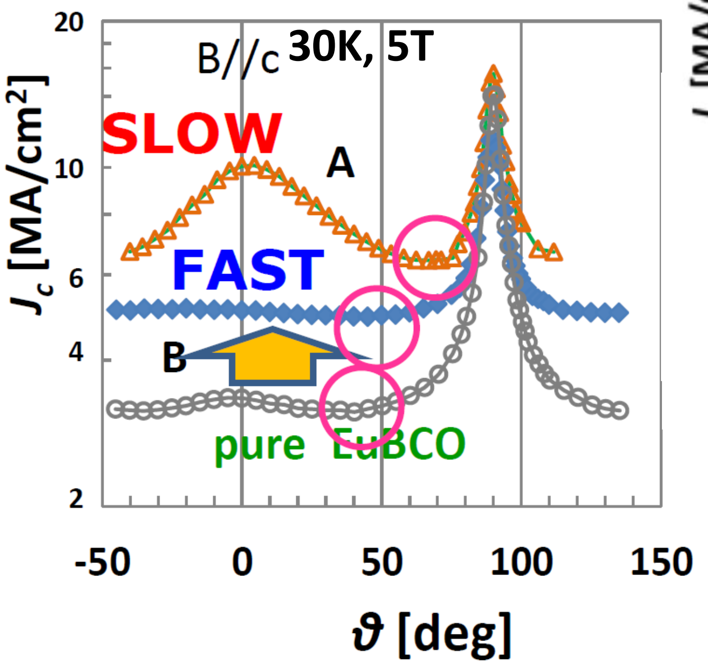

Y. Iijima, CCA 2023

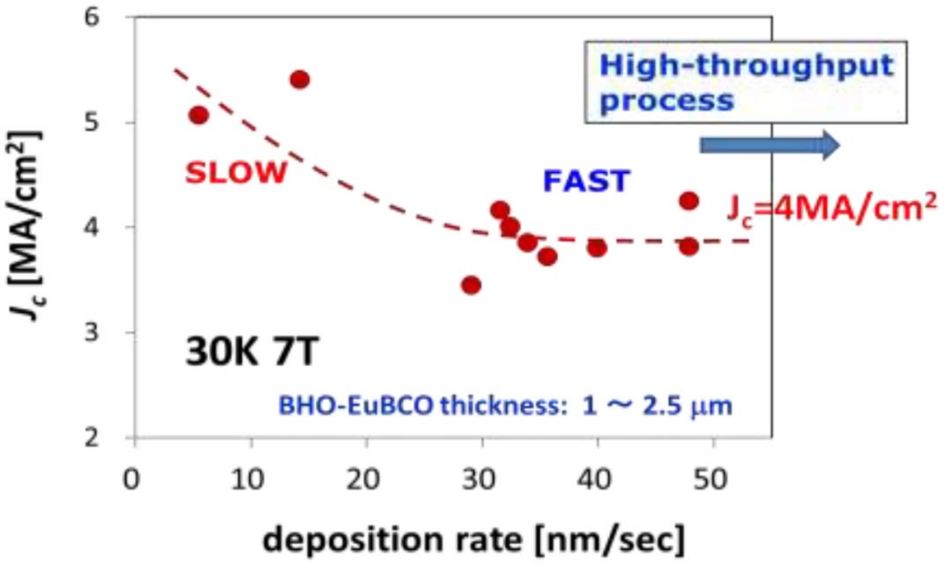

Aligned long nanorods are not essential at low T - high H

FARADAY FACTORY JAPAN

YBCO + Y_2O_3 nanoparticles

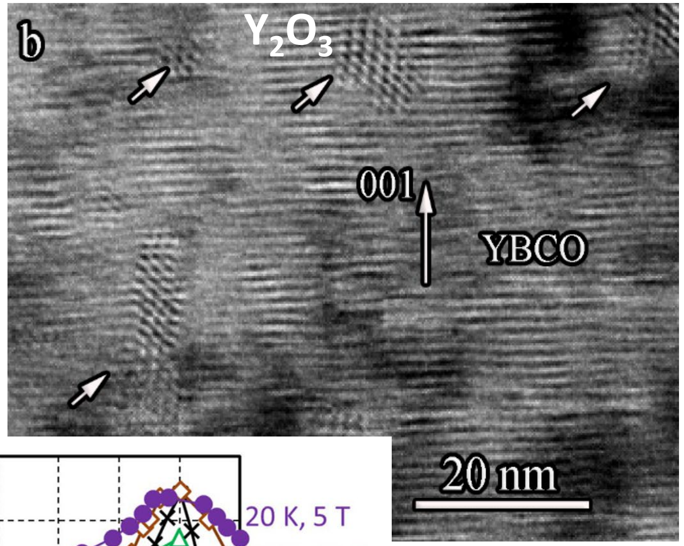

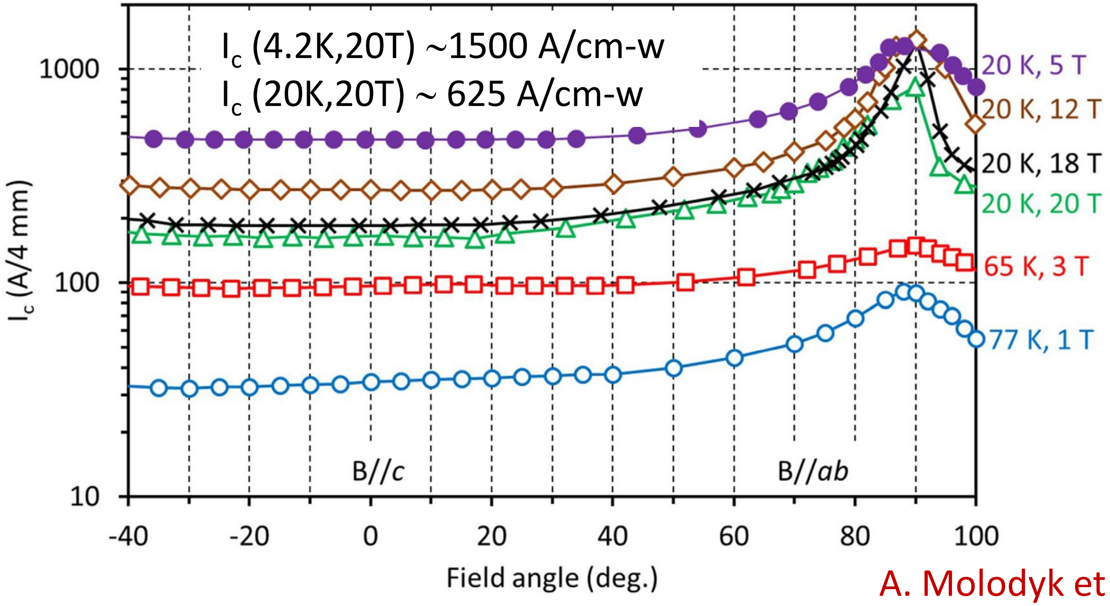

A. Molodyk et al, Sci. Rep 11 (2021)

Nanostrain is the most relevant parameter controlling single vortex pinning (CSD-TFA and CSD-TLAG)

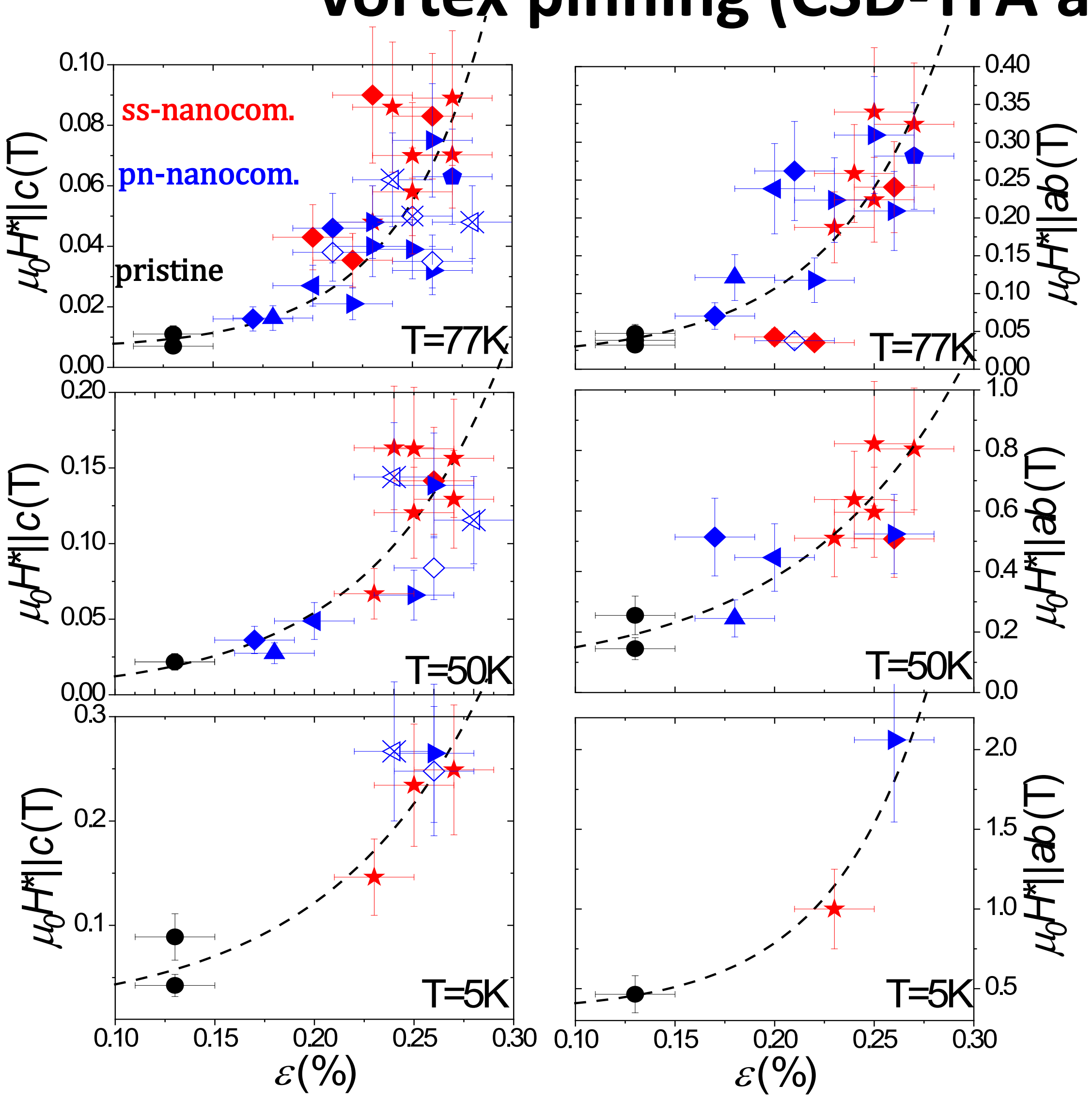

H* enhanced by nanostrain H//c and H//ab

F. Vallés et al, Comm Mat 3,45 (2022)
Z. Li et al., Sci Rep (2019)

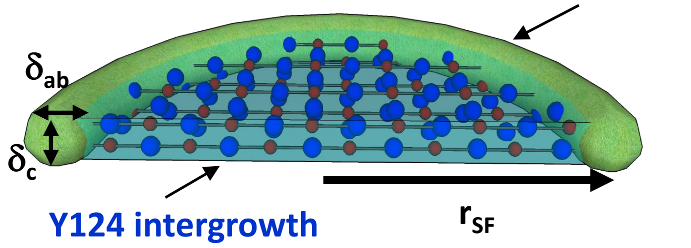

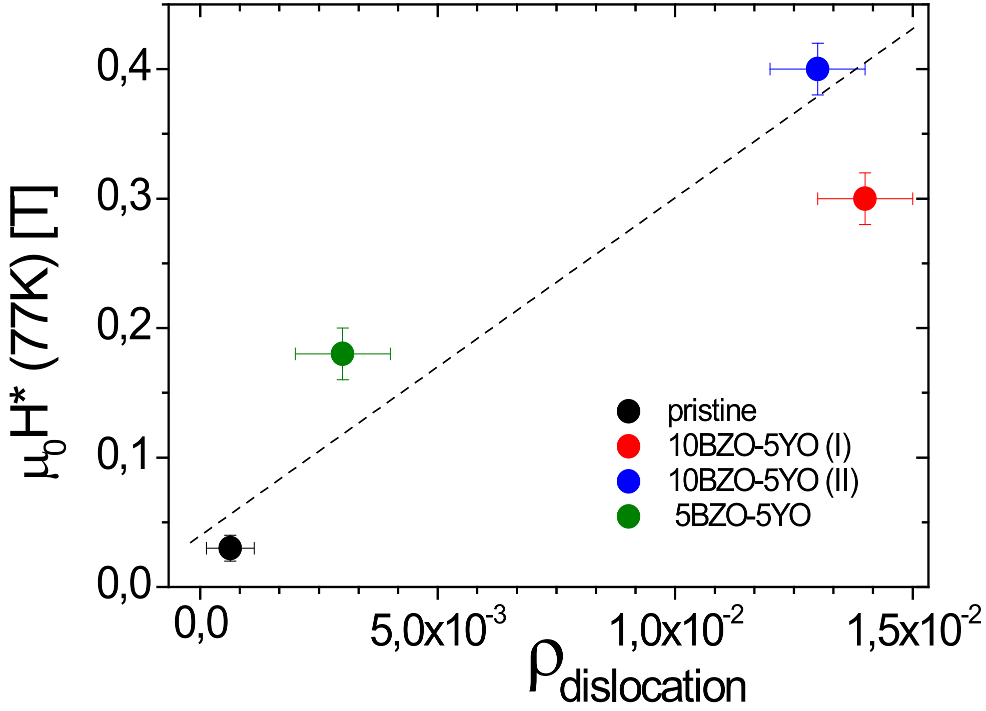

Close relationship among dislocation density and nanostrain

Synergistic combination of Nps and nanostrain: enhanced vortex pinning

CTA: Conventional Thermal Annealing (0.4 ºC/s)
FH: Flash heating (20ºC/s) - Enhanced vortex pinning

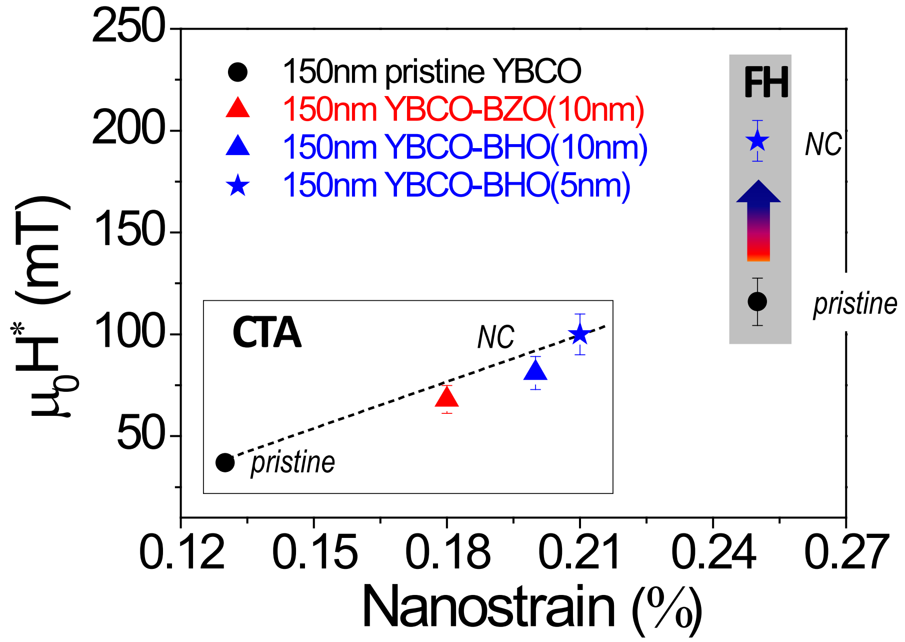

TFA

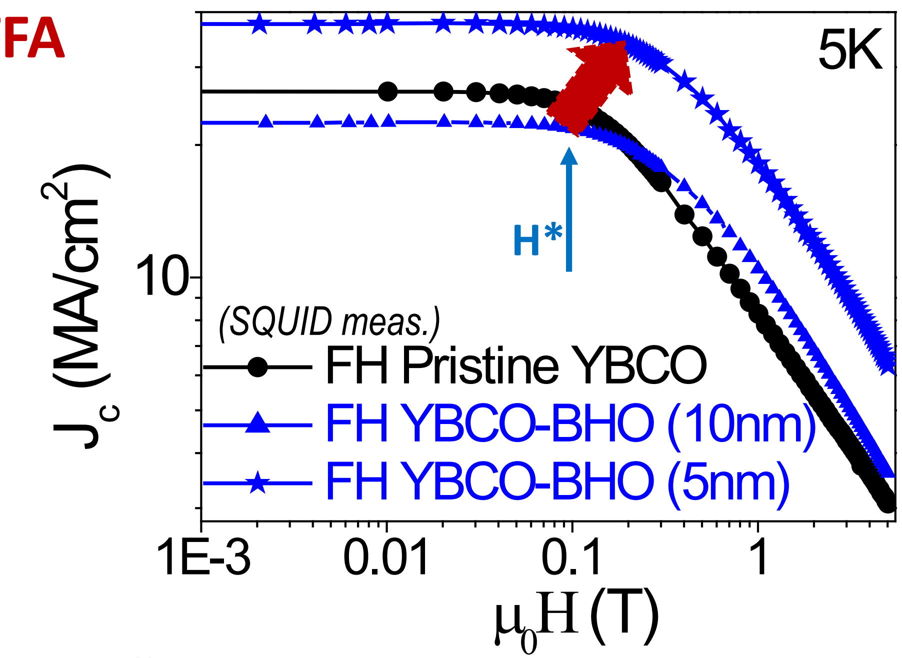

A leap increase of H* beyond nanostrain
NP diameter ~ξ_{ab} (coherence length)

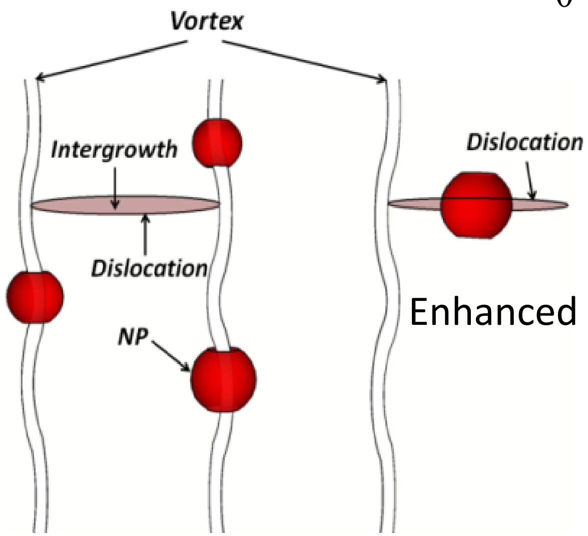

Enhanced vortex pinning

Nanostrain & NPs (4-8 nm): Synergistic effect for enhanced vortex pinning

Z. Li et al, Sci Rep. (2019)
Z. Li et al, J Mat Chem C (2019)
A. Palau et al., SUST (2018)

Enhanced vortex pinning by nanoparticles (UTOC)

CSD-TFA growth: (Y,Gd)$Ba_{1.5}Cu_3Ox$ / BHO

$$J_{co}^{NPs} \propto N_{np} \frac{\mu_o H_c^2 \pi \xi^2 D}{4\xi} \propto N_{np}\left(\frac{1}{\lambda^2 \xi}\right)$$

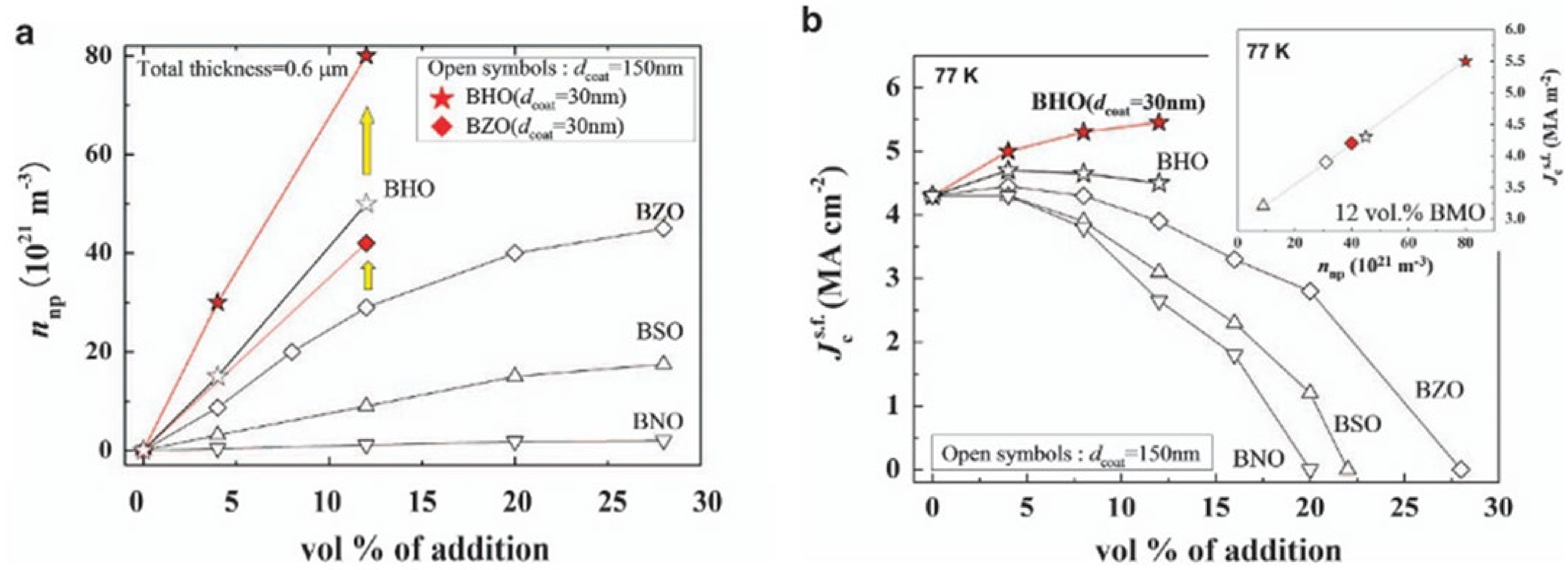

Very small BHO NPS achieved with UTOC (~ 7 nm) with coatings of 30 nm

Very small BHO NPs contribute as APCs

M. Miura et al., NPG Asia Materials (2017)

Anisotropy of superconducting properties

Effective anisotropy decrease due to nanostrain (SFs) and nanoparticles

$$\epsilon_{\text{eff}}(\theta) = [\cos^2\theta + \gamma_{\text{eff}}^{-2}\sin^2\theta]^{1/2}.$$

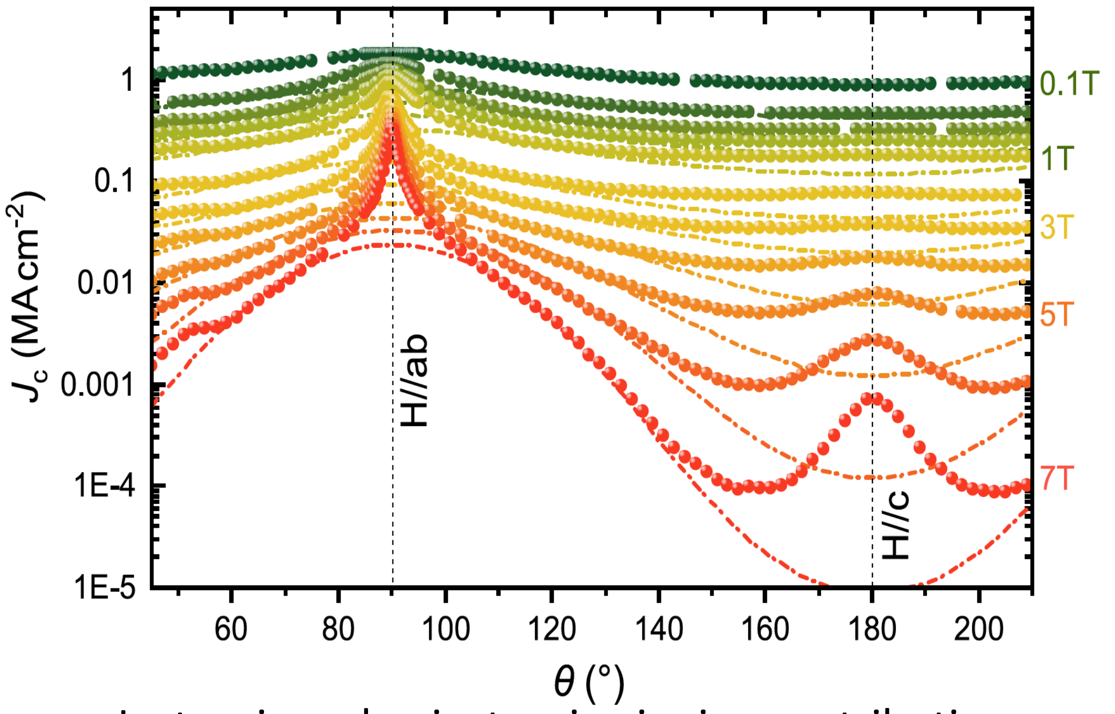

Isotropic and anisotropic pinning contributions

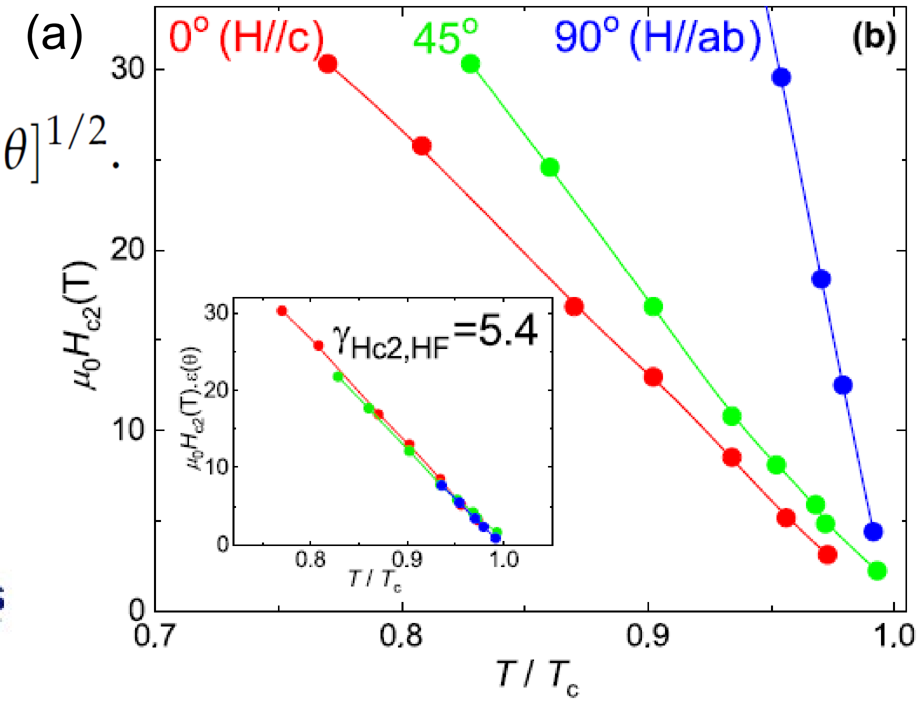

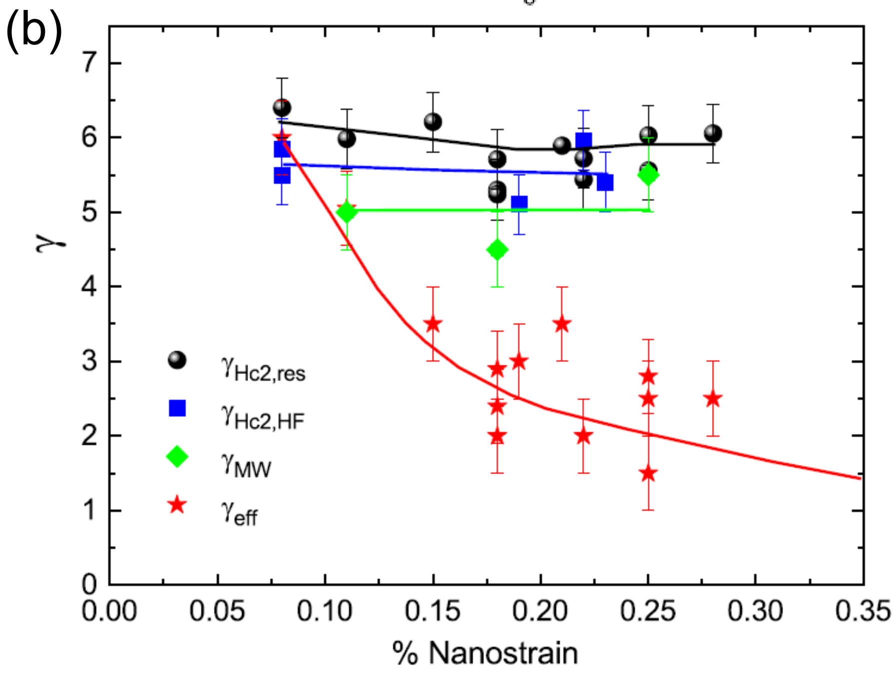

L. Soler et al, Nature Communications (2020)
E. Bartolomé et al., Phys Rev B (2019)
N. Pompeo et al., SUST (2020)
J. Banchewski et al, to be published

Anisotropy of superconducting properties

Effective anisotropy decrease due to nanostrain (SFs) and nanoparticles

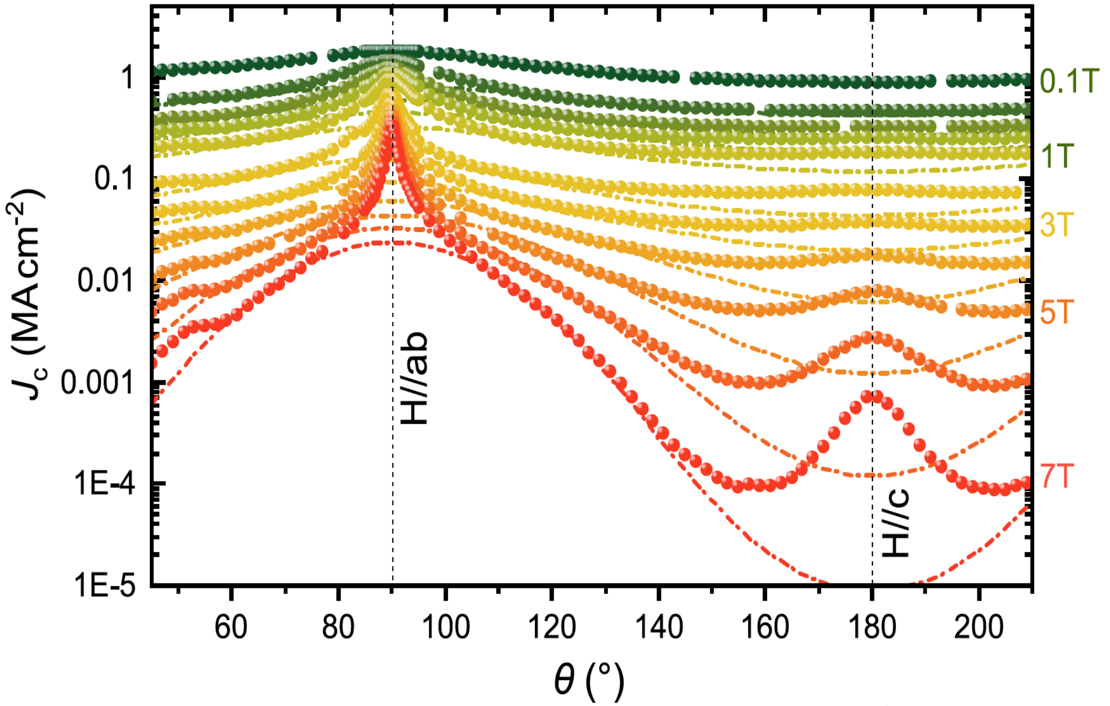

Isotropic and anisotropic pinning contributions

Los Alamos NATIONAL LABORATORY

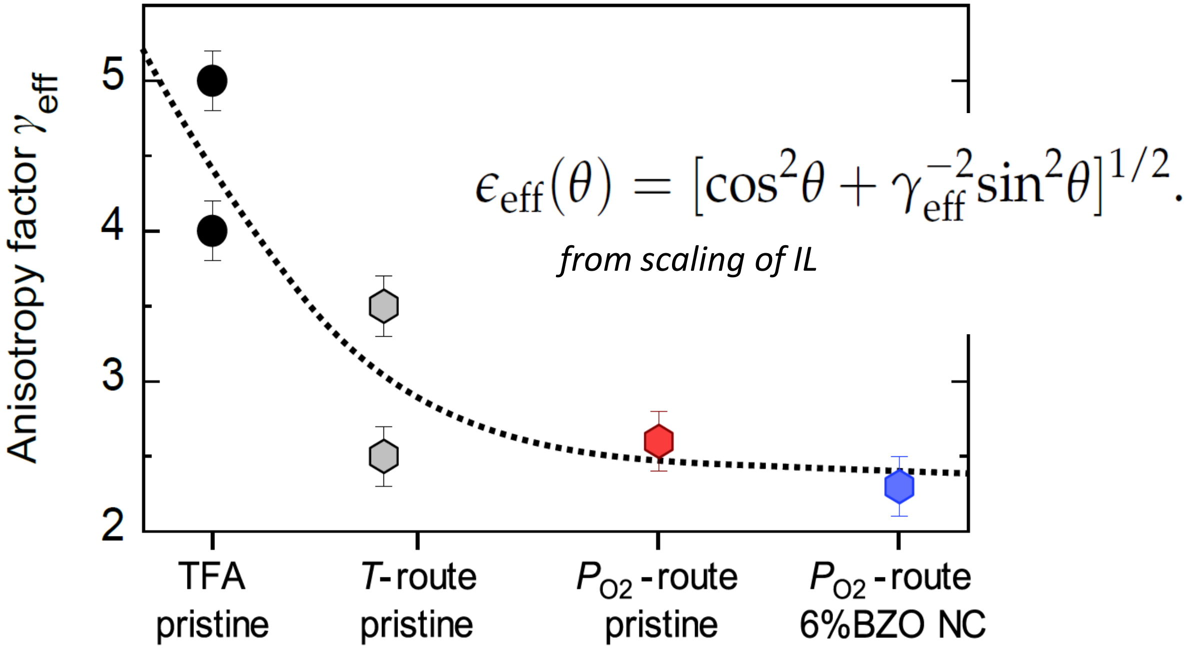

L. Soler et al, Nature Communications (2020)

E. Bartolomé et al., Phys Rev B (2019)

N. Pompeo et al., SUST (2020)

J. Banchewski et al, to be published

Strong/Weak Vortex Pinning Contributions: temperature dependence

$$J_c(T) = J_c^{\text{iso-wk}}(T) + J_c^{\text{iso-str}}(T) + J_c^{\text{aniso-str}}(T)$$

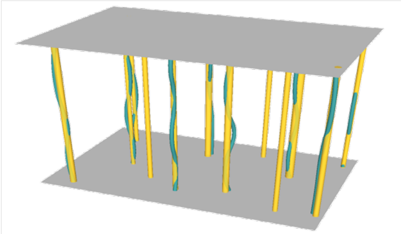

Anisotropic strong

- Nanorods (H//c)
- Intrinsic Pinning (H//ab)
- Stacking faults (H//ab)
- Twin boundaries (H//c)

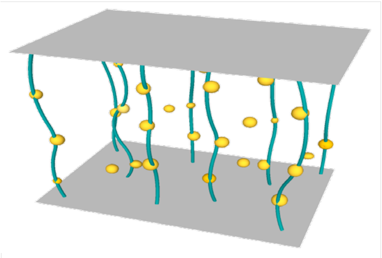

Isotropic strong

- Nano-strain
- Nanoparticles

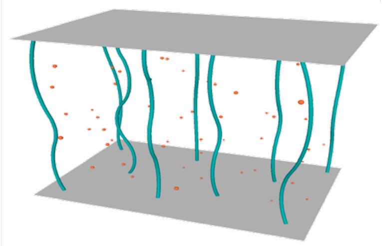

Isotropic weak

- Point defects, Oxygen and cationic vacancies

$$J_c^{strong}(T) = J_c^{str}(0) exp\left[-3\left(\frac{T}{T^*}\right)^2\right]$$

$J_c^{str}(0)$ → density of strong defects

T^* → characteristic vortex pinning energy of strong defects

$$J_c^{weak}(T) = J_c^{wk}(0) exp\left(-\frac{T}{T_0}\right)$$

$J_c^{wk}(0)$ → density of weak defects

T_0 → characteristic vortex pinning energy of weak defects

We can quantify the pinning strength and energies associated to different pinning centres

We assume additive effects of strong and weak APCs

D.R.Nelson and V.M.Vinokur: PRL, **68**: 2398 (1992) **;** PRB, **48**: 13060 (1993)
G.Blatter.et.al., RMP, **66**: 1125 (1994)

Strong/Weak/Isotropic-Anisotropic Vortex Pinning Contributions: temperature dependence

Considering the same density of defects ($J_c(0)$)

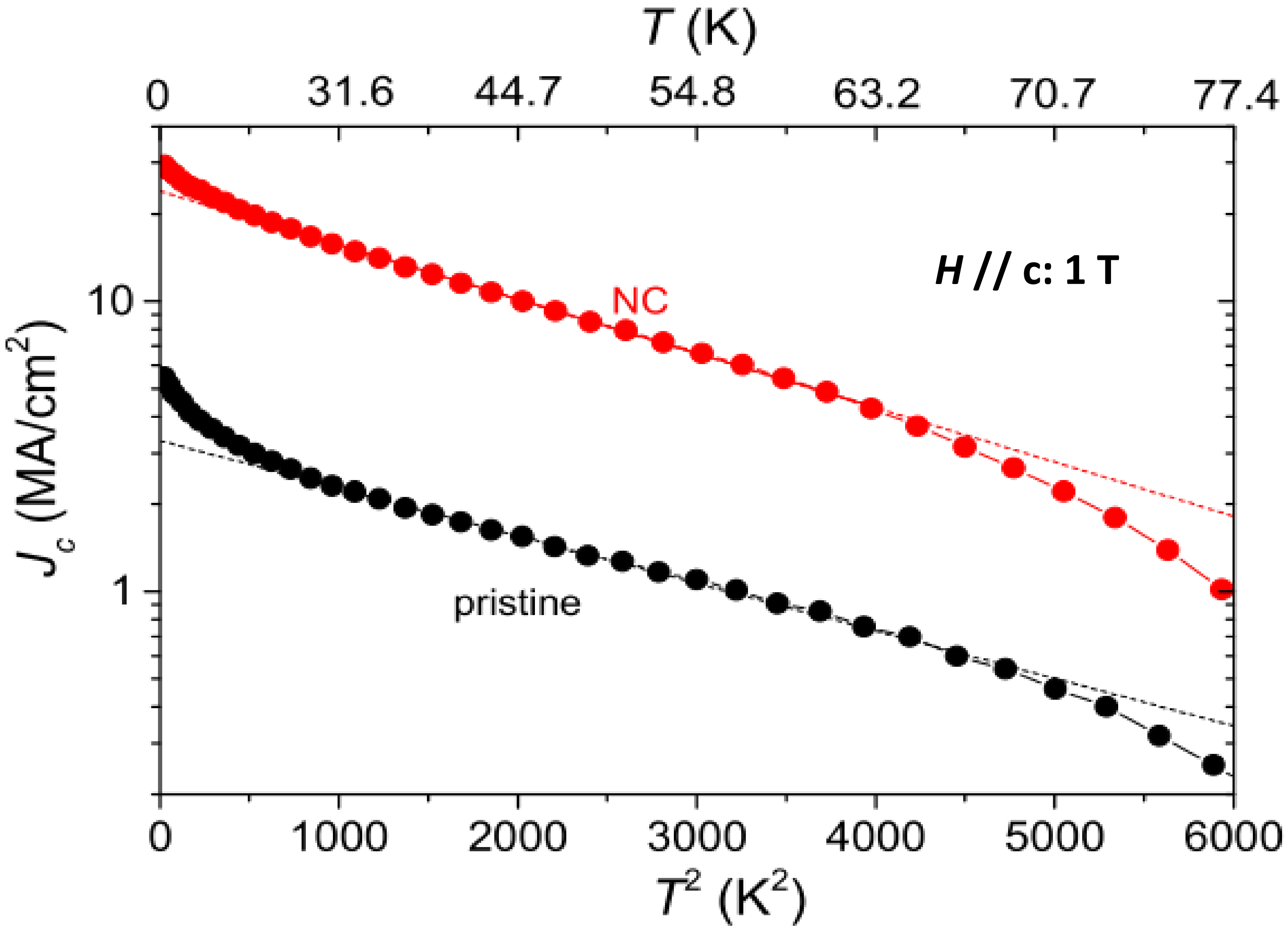

Pinning contributions in nanocomposite films: very high magnetic fields (35 T)

ICMAB INSTITUT DE CIÈNCIA DE MATERIALS DE BARCELONA
EXCELENCIA SEVERO OCHOA
NATIONAL HIGH MAGNETIC FIELD LABORATORY

$$J_c(T) = J_c(0)^{\text{iso-wk}} \exp(-T/T_0) + J_c(0)^{\text{iso-str}} \exp(-3(T/T^*_{\text{iso-str}})^2) + J_c(0)^{\text{aniso-str}} \exp(-3(T/T^*_{\text{aniso-str}})^2)$$

D. Abraimov
J. Jaroszynski
D. Larbalestier

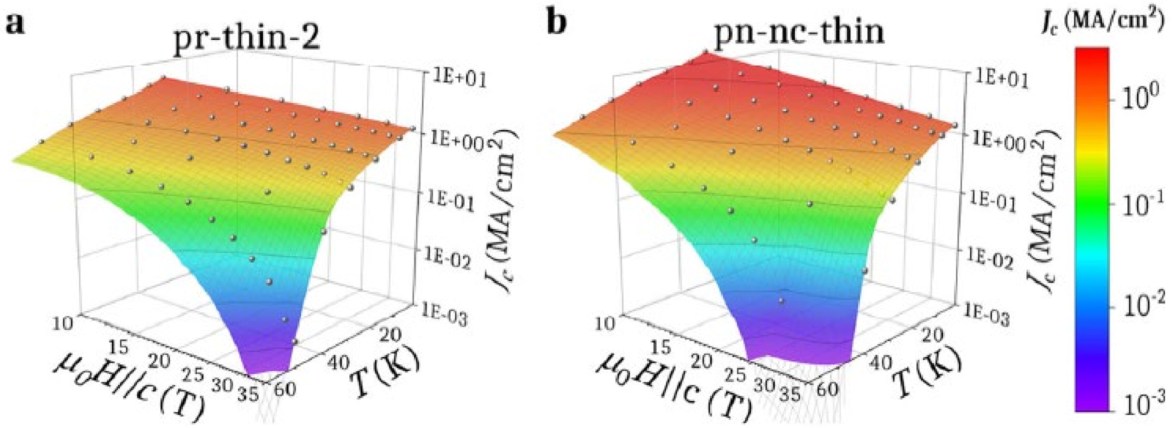

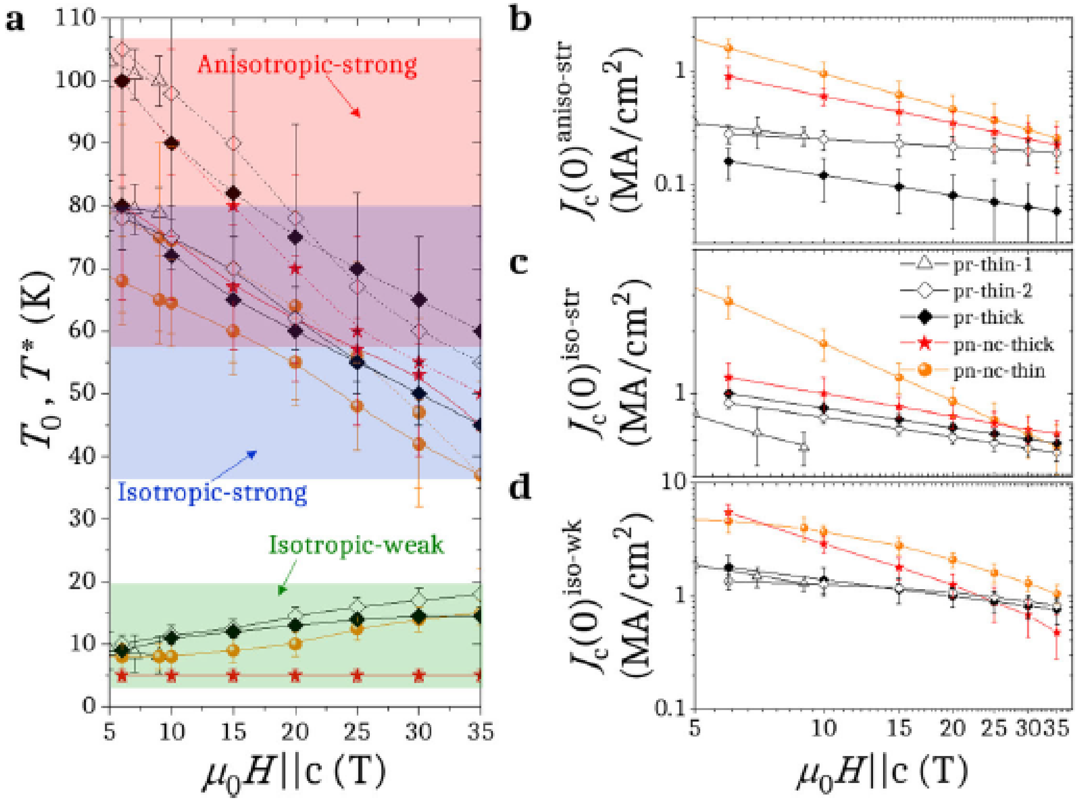

- Very different magnetic field dependences for weak and strong pinning defects
- Weak pinning defects may play a critical role at very high magnetic fields and low temperatures

F. Vallés et al, Comm Mat 3,45 (2022)

Phase diagrams of vortex pinning strength

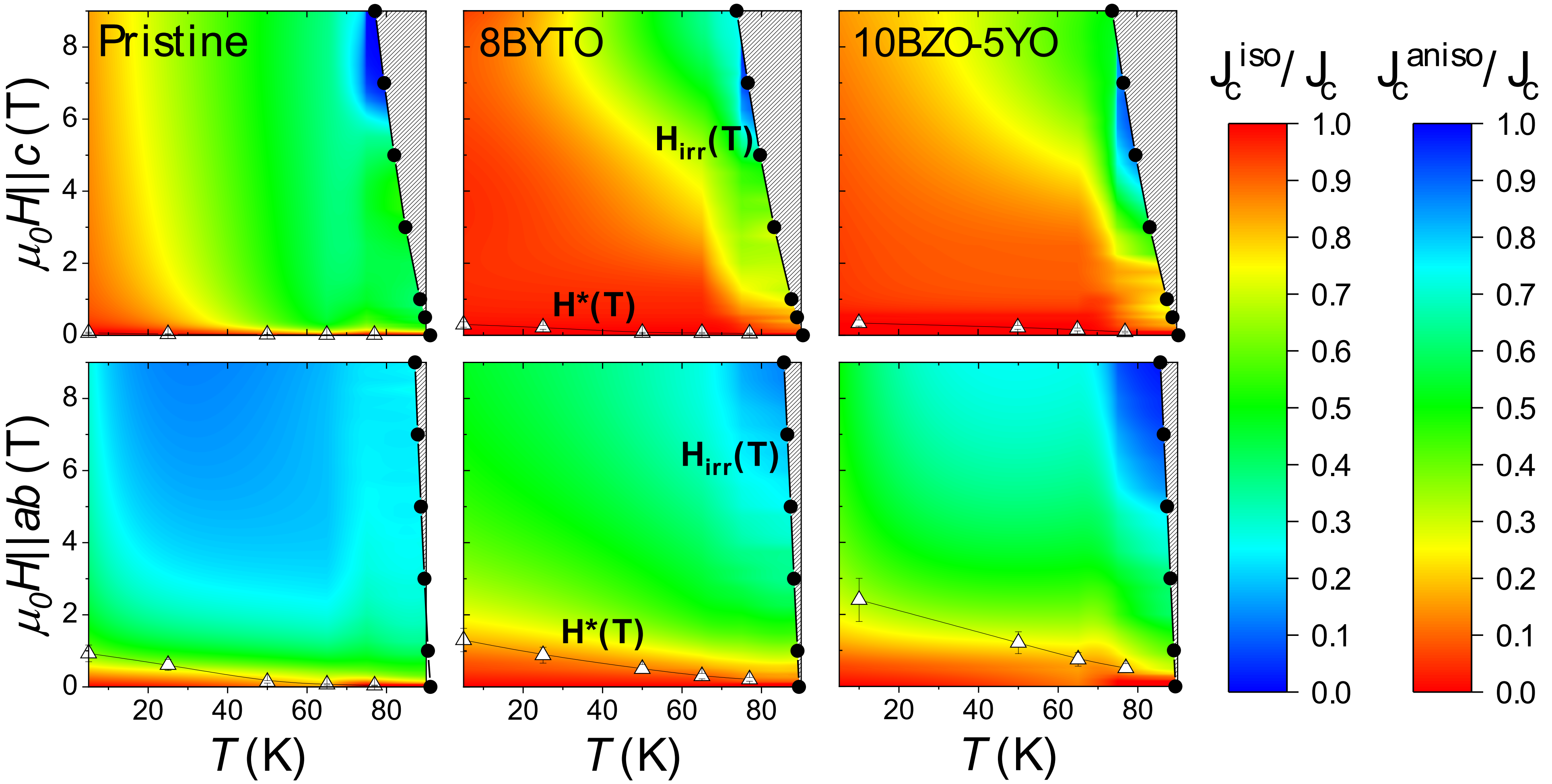

CSD nanocomposites: Single Vortex Pinning vs collective pinning

- **Isotropic pinning dominates most of phase diagram (H//c)**
- **Isotropic and anisotropic pinning with similar relevance in most of the phase diagram (H//ab)**

Vortex pinning consequences at high growth rate: TLAG-CSD

50 nm/s → 1500 nm/s

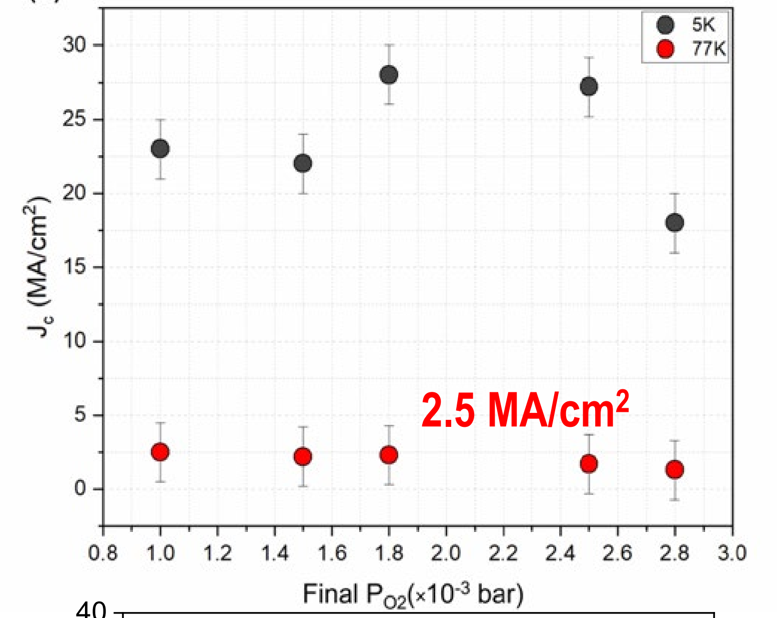

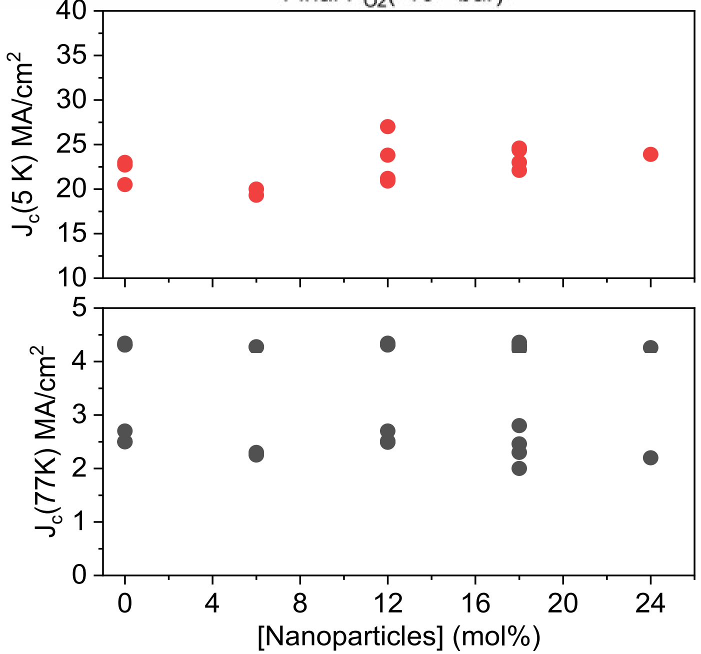

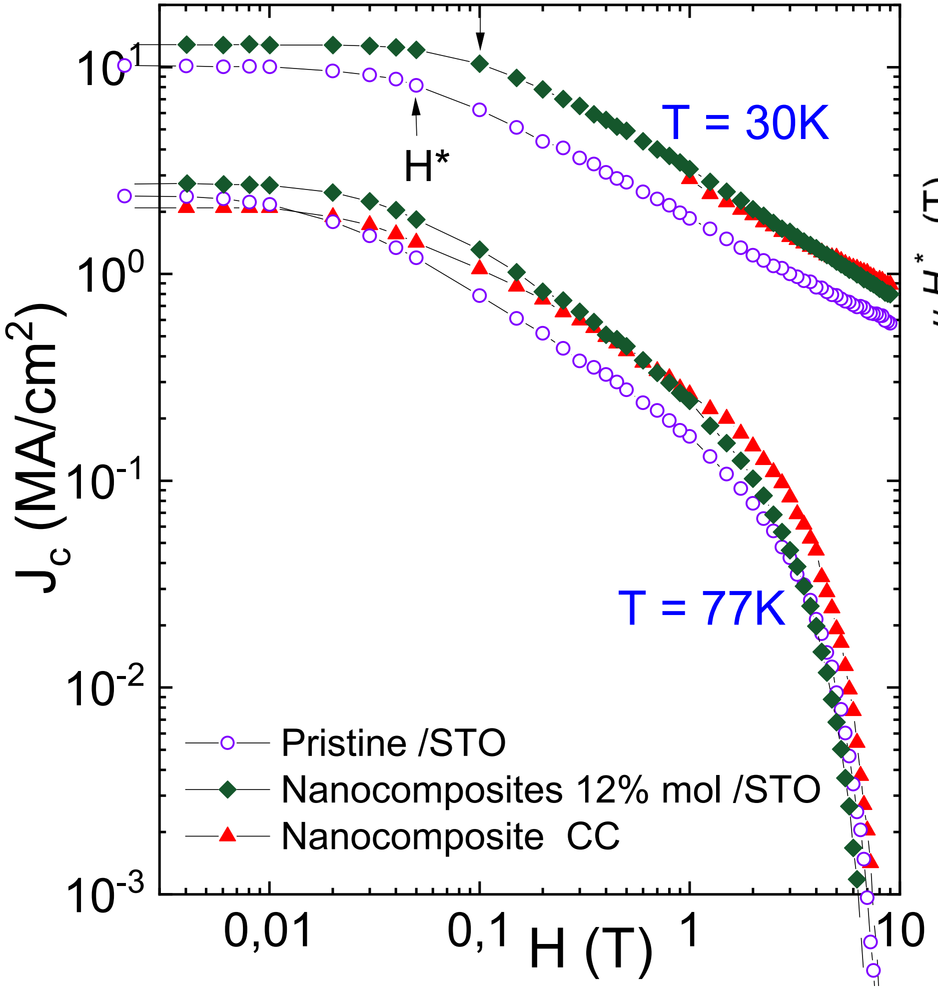

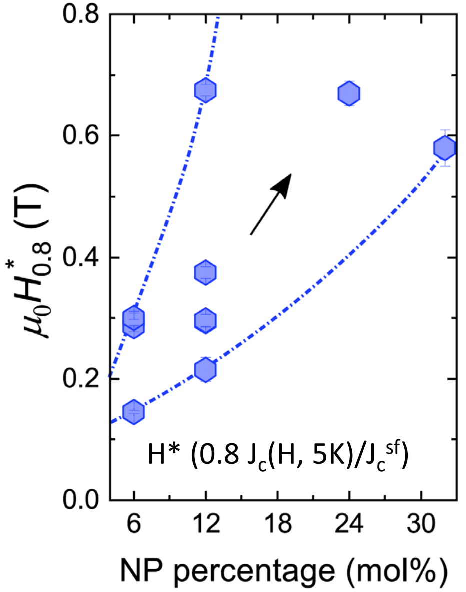

Rich vortex pinning determined by the defect microstructure of high growth rates

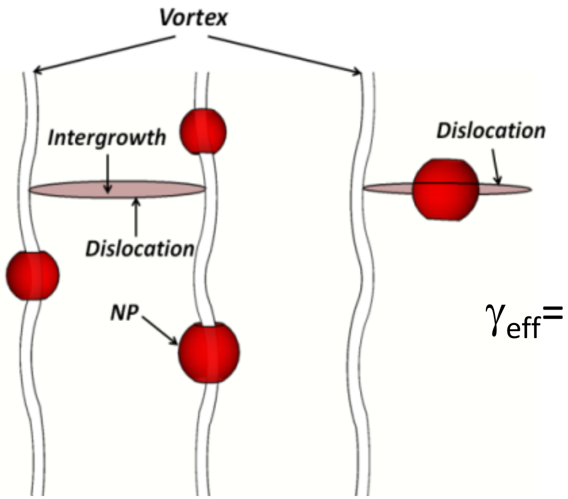

γ_{eff}= 2-2.5

L. Soler et al., Nat Comm (2020), S. Rasi, et al, Advance Science (2022)

Tune charge carrier density by oxygen overdoping

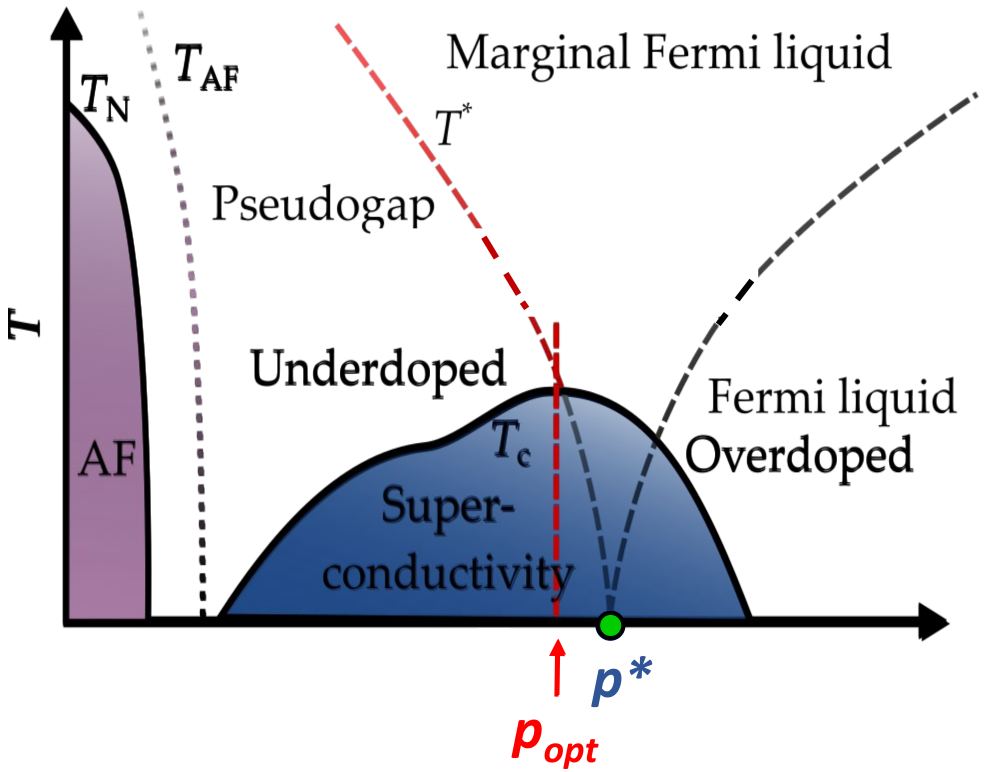

p_{opt} = 0.16 holes/CuO_2-plane: optimal doping for maximum T_c

p^*= 0.19 holes/CuO_2-plane: Critical doping (QCP)

Pinning force $\boldsymbol{F_p} = \sum_i^{N_p} f_{p,i}\,(B,T) \propto \boldsymbol{J_c}$

$f_p \propto \boldsymbol{E_c}$ condensation energy

$\boldsymbol{J_d^2} \propto n_s \boldsymbol{E_c} \longrightarrow \boldsymbol{J_c^2} \propto \boldsymbol{n_H H_0}$ (H_0 from in-plane magnetoresistance)

(three independent experimental parameters)

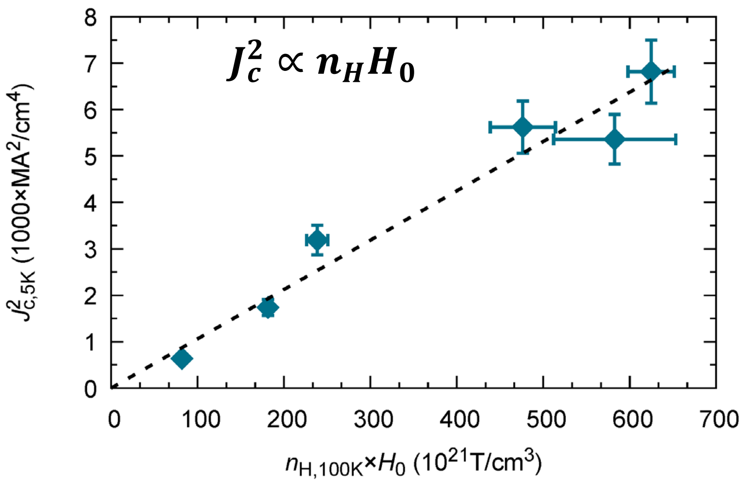

$\boldsymbol{n_H}$ and $\boldsymbol{E_c}$ increases in the overdoped state, and consequently $\boldsymbol{J_c}$ should increase

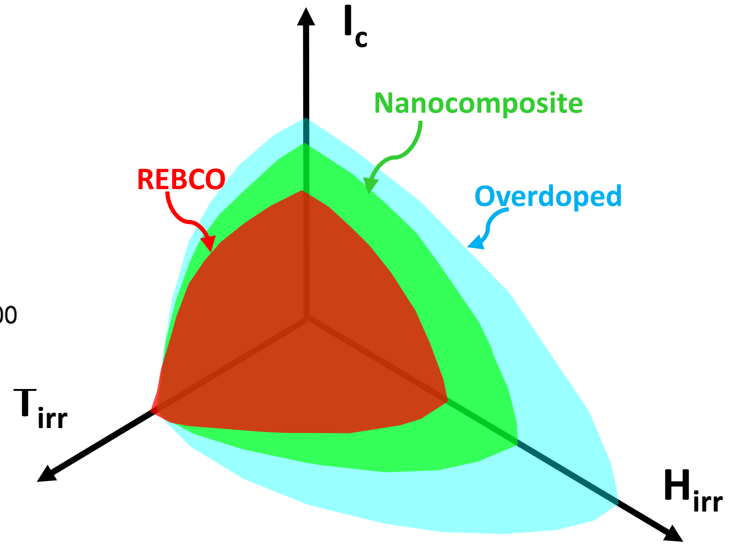

A. Stangl et al, Sci. Rep. (2021)

Carrier concentration effects: oxygen overdoping

YBCO PLD and TFA – CSD thin films

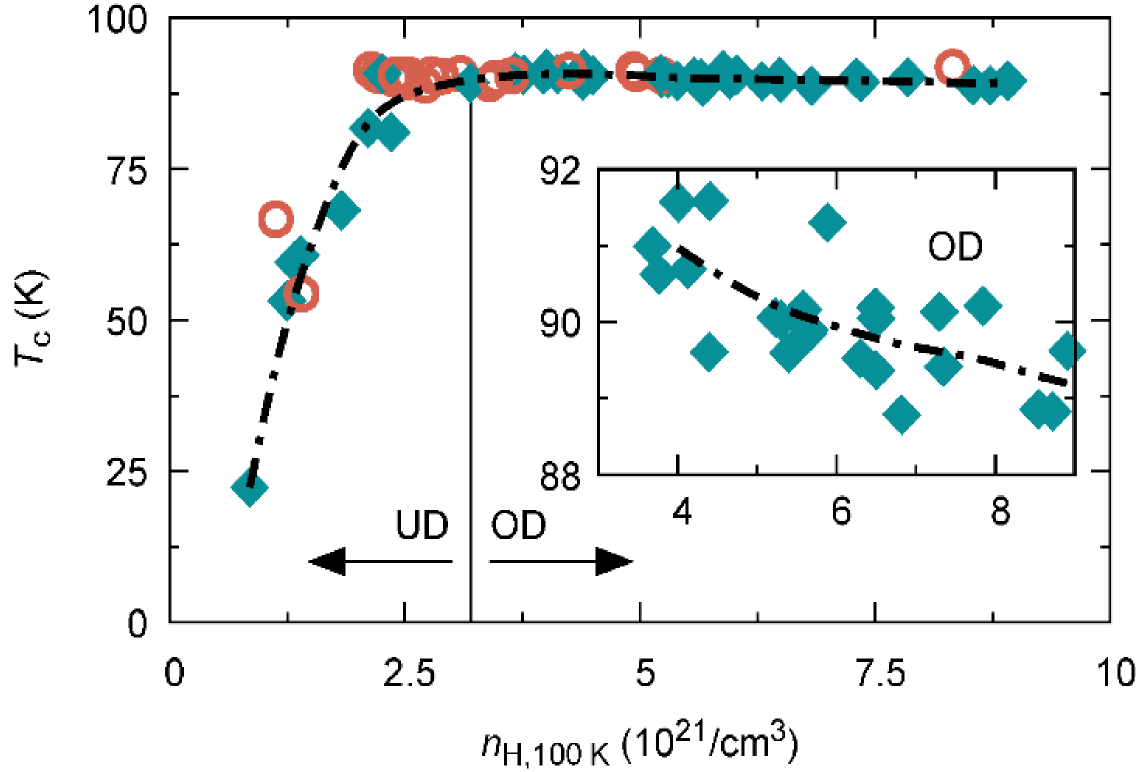

- Carrier concentration determined by Hall effect (100 K)
- Overdoping is achieved by oxygen excess

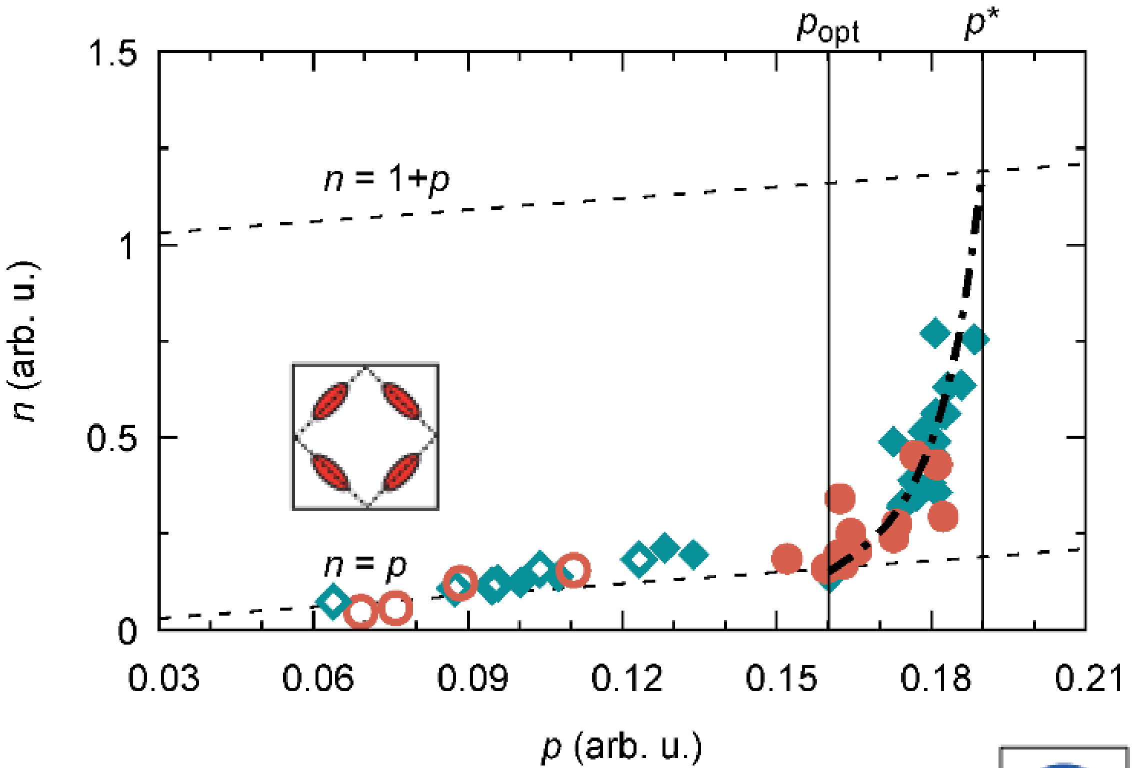

- Fermi surface reconstruction at the Quantum Critical Point ($p^* > p_{opt}$): large increase of the carrier density n (cylindrical Fermi surface)
- Non-unique relation between the charge carrier density n and doping, p.

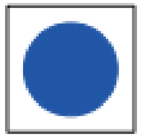

A. Stangl et al, Sci Rep (2021)

Proust, C. & Taillefer, L. T, *Annu. Rev. Condens. Matter Phys.* **10**, 409 (2019)

Strong increase of J_c in the overdoped state

ICMAB
INSTITUT DE CIÈNCIA DE MATERIALS DE BARCELONA
EXCELENCIA SEVERO OCHOA

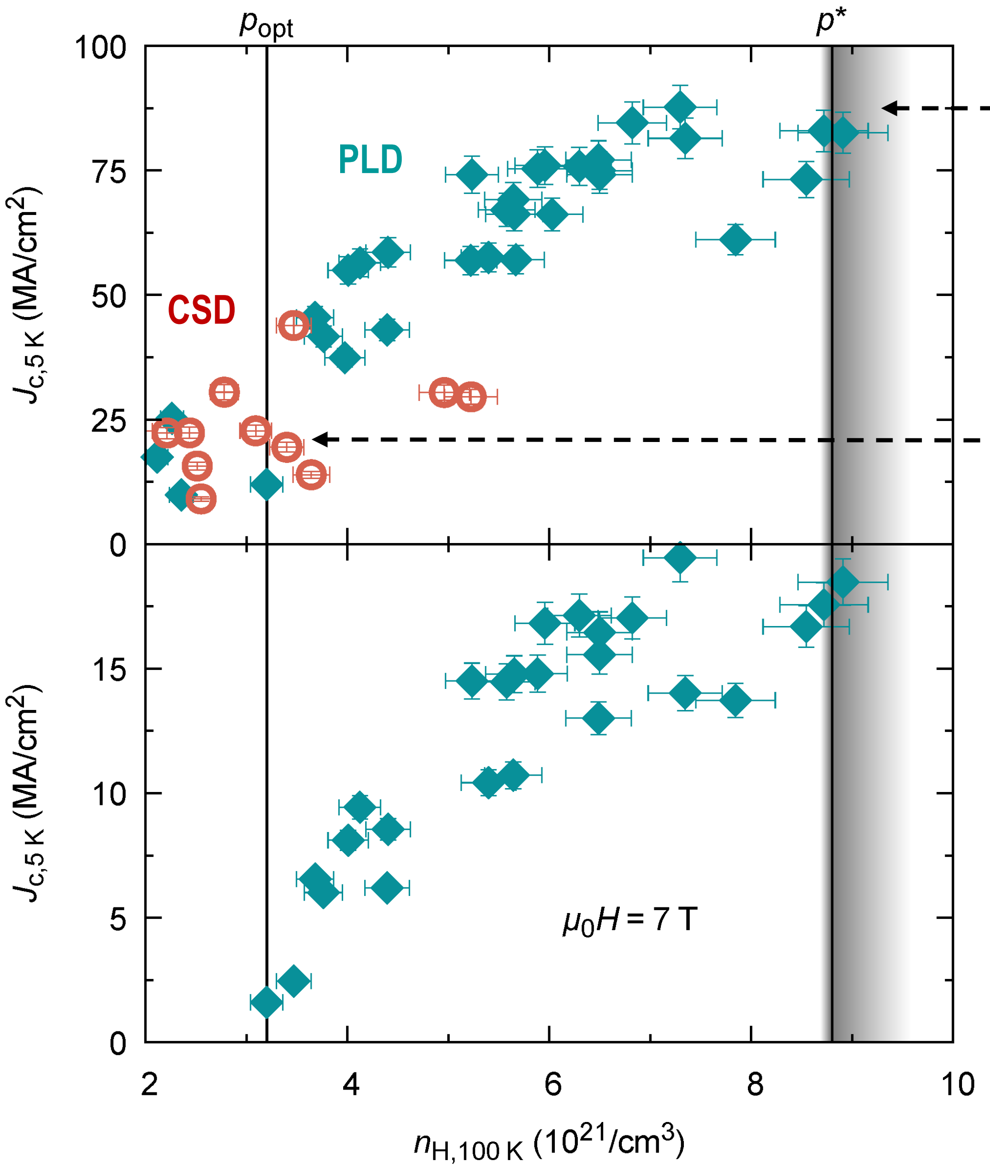

$$J_c(p^*) \approx \frac{1}{5} J_d(p^*) = 90\ MA/cm^2$$

$J_d(p^*) \approx$ 500 MA/cm²

$$J_c(p^{opt}) \approx \frac{1}{10} J_d(p^{opt})$$

$J_d(p^{opt}) \approx$ 330 MA/cm²

TEL AVIV UNIVERSITY

Strong increase of J_c with n_H
(x4 from p_{opt} to p*)

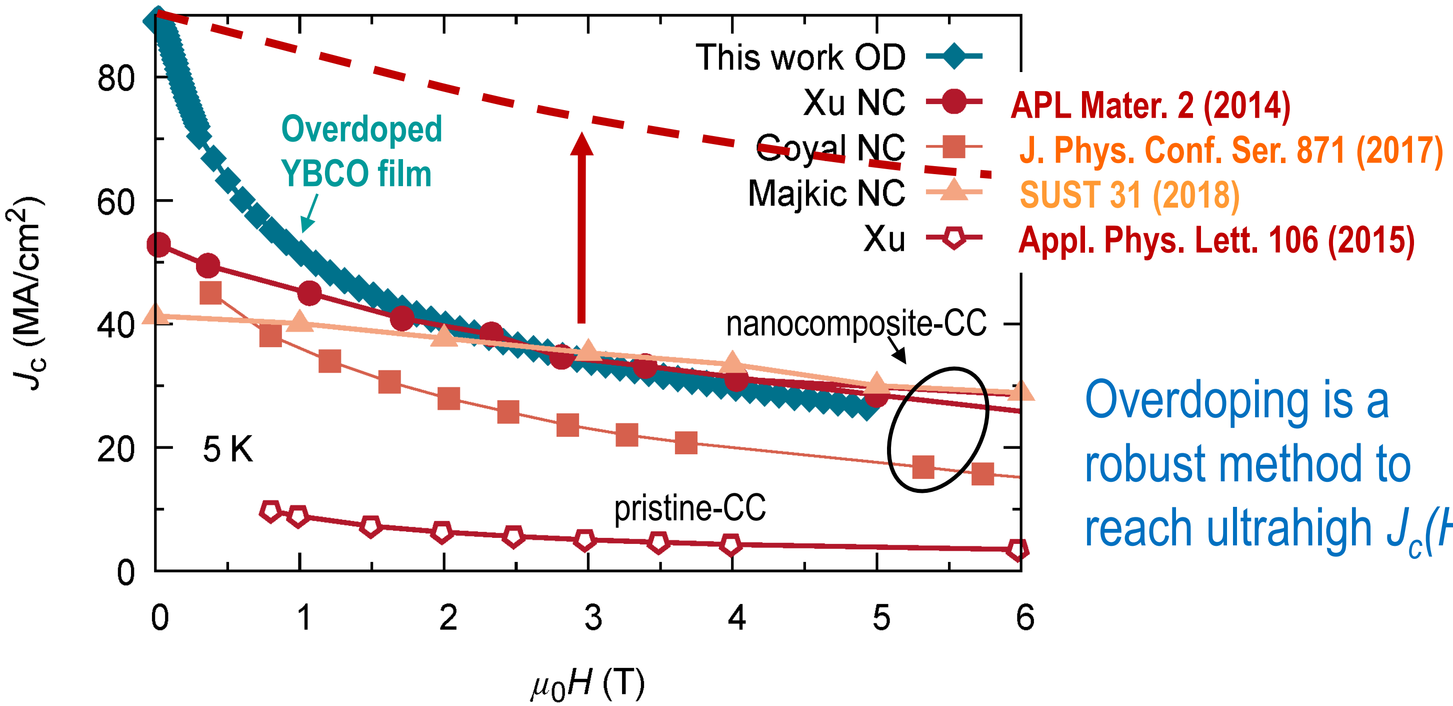

Overdoping is a robust method to reach ultrahigh $J_c(H)$

A. Stangl et al, Scientific Reports (2021)

Strong increase of J_c in the overdoped state of nanocomposites

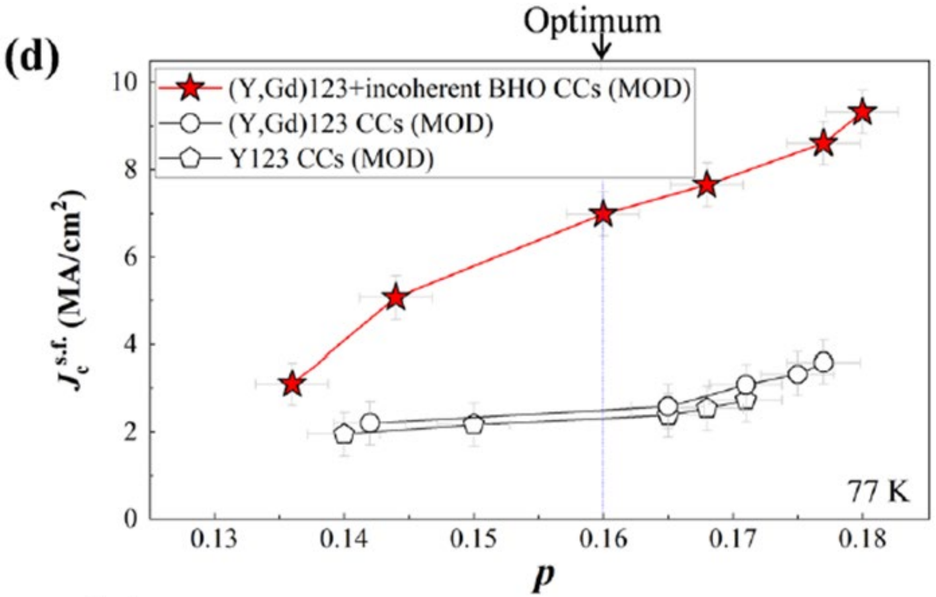

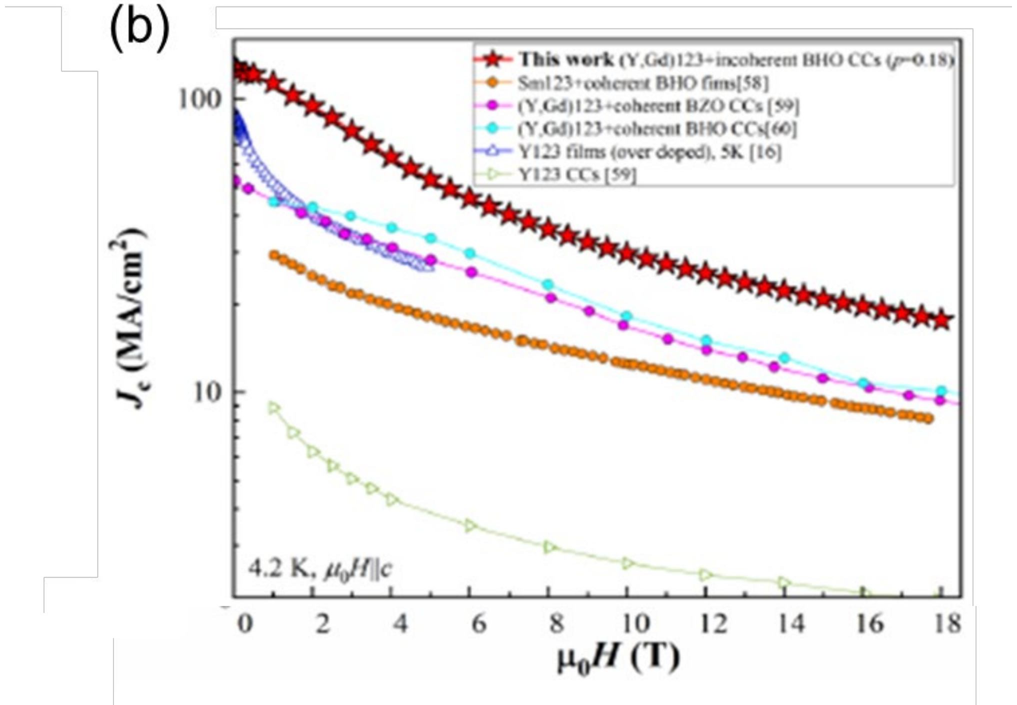

$$J_{co}^{NPs} \propto N_{np} \frac{\mu_o H_c^2 \pi \xi^2 D}{4\xi} \propto N_{np} \left(\frac{1}{\lambda^2 \xi}\right)$$

- Nanoparticles increase of J_c^{sf}
- Influence of carrier concentration through thermodynamic parameters

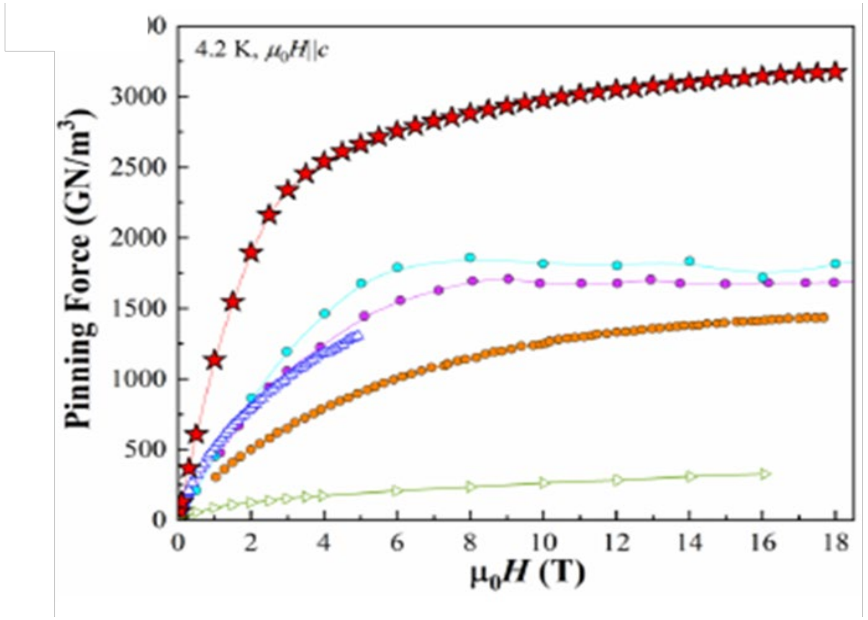

M. Miura et al, NPG Asia Materials (2022)
TFA-REBCO film growth with UTOC nanoparticles

Strong increase of J_c in the overdoped state of nanocomposites

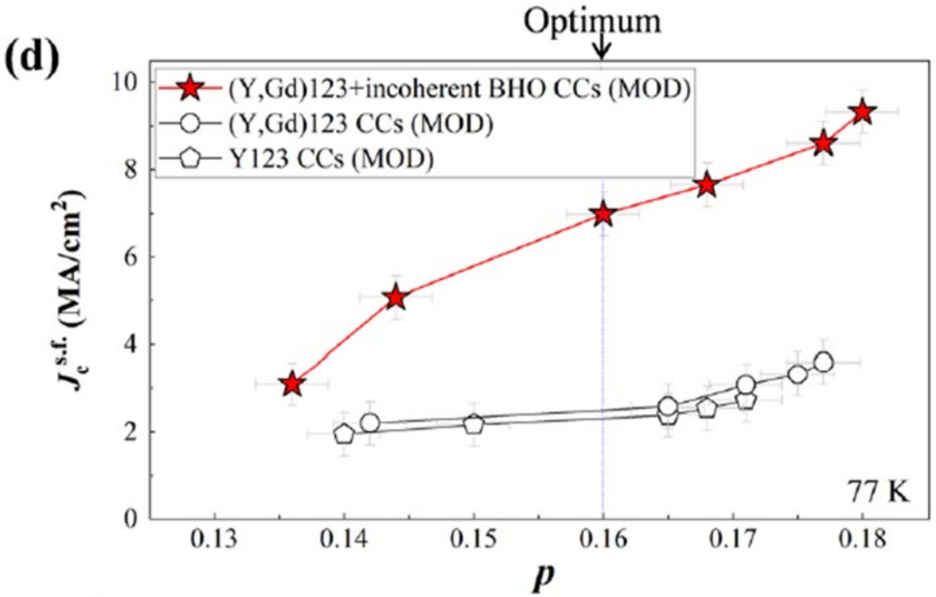

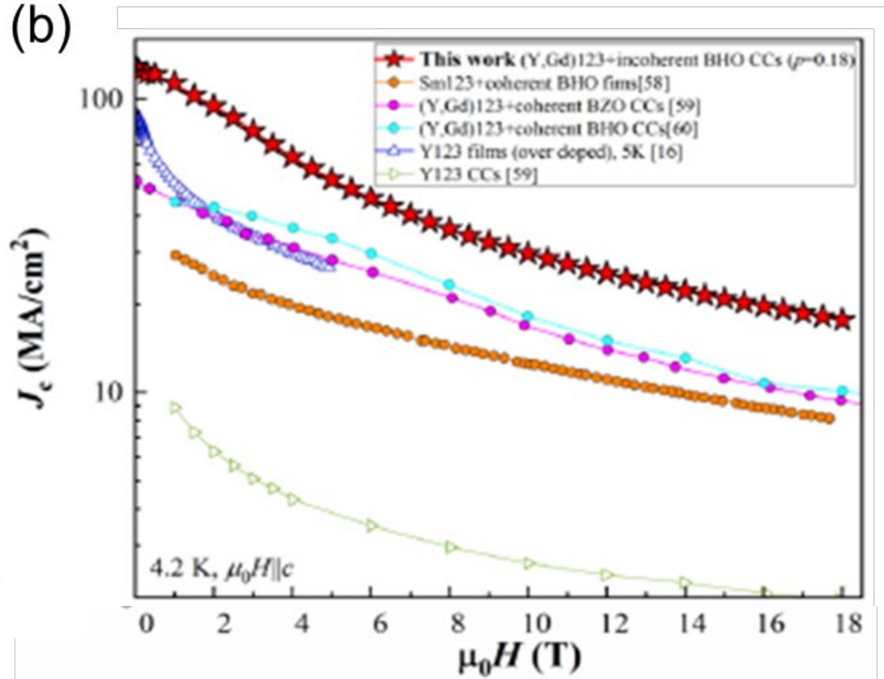

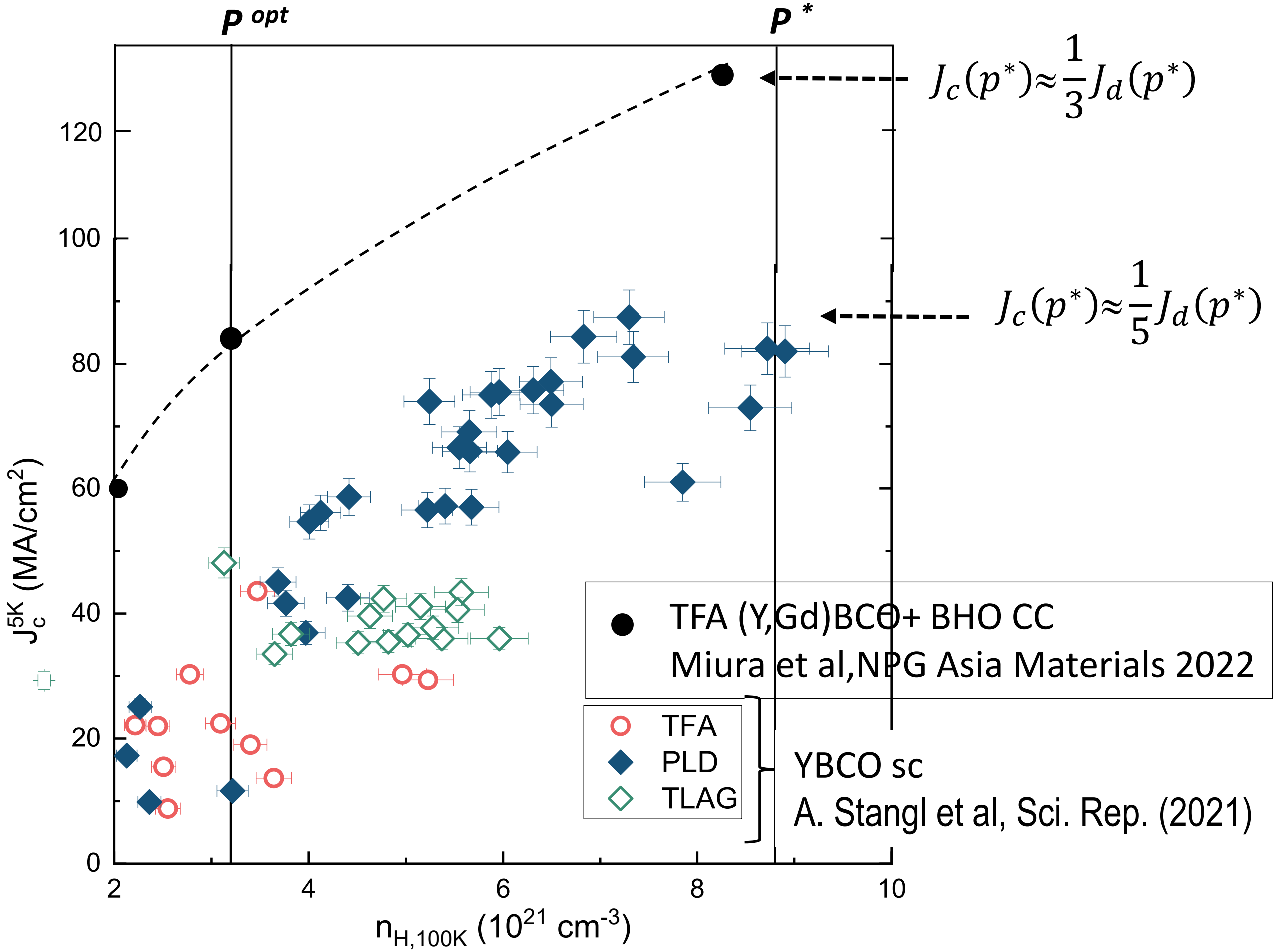

Comparison between different growth processes

Film features	Growth from vapour	Growth from liquid	Growth from solid
Growth mechanism	Gas–solid transformation	Liquid–solid transformation	Solid–solid transformation controlled by gas diffusion
Growth rate	Medium (≈0.5–25 nm s^{-1})	Ultra-fast (≈100–2.000 nm s^{-1})	Slow (0.5–3 nm s^{-1})
Supersaturation control	Deposition rate, T, P_{O2}	RE ion, liquid composition, T, P_{O2}	P_{H2O}, T, P_{O2}
Deposition and growth environment	Simultaneous deposition and growth: PLD, MOCVD, ME; high-vacuum environment	Sequential deposition and growth; atmospheric and intermediate pressures (TLAG-CSD); high-vacuum and intermediate pressures (RCE-DR)	Sequential deposition and growth; atmospheric pressure deposition (TFA-CSD, BaF_2); growth at normal or slightly reduced pressures
Precursors	Targets (PLD, ME); volatile metalorganics (MOCVD)	Fluorine-free metalorganic solutions; evaporated metals (RCE-DR)	Fluorine-based metalorganic solutions (TFA-CSD); evaporated metals (BaF_2)
Nanocomposites: second-phase nanostructures	Self-assembled nanorods, nanoparticles	Spontaneous segregation, preformed nanoparticles	Spontaneous segregation, preformed nanoparticles
Nanostructures orientation	Epitaxial	Epitaxial or random	Random
Main vortex pinning centres	Nanorods, nanoparticles, point defects	Nanostrain, nanoparticles, point defects, twin boundaries	Nanostrain, nanoparticles, point defects, twin boundaries
Critical current (A/cm-width) industrialized values	1,000–1,600 at 4.2 K, 20 T; 350–700 at 20 K, 20 T; 350–750 at 77 K, 0 T		
Large-scale manufacturing	Medium throughput, high CAPEX	High throughput, large areas, simplified furnaces, low CAPEX	Low throughput, complex furnaces, small areas, low CAPEX
Potential cost, performance	Medium	Low	Medium

T. Puig, J. Gutiérrez, X. Obradors Nat Rev Phys (2023, doi.org/10.1038/s42254-023-00663-3)

Conclusions and take away message

- Coated conductors are unique superconducting materials that are set to enable UHF magnets for compact fusion
- Very long lengths of CCs are required so high throughput production is required at low cost keeping high performance
- Ultrafast REBCO growth rates are required to reduce the figure of merit cost/performance (€/kA m)
- Nanostructure deeply differs beween simultaneous and sequential deposition and growth methodologies
- Reliable and fast characterization methodologies are required to identify the efficient APCs at different temperatures and magnetic fields
- Liquid assisted growth methodologies are very promising to increase throughput
- TLAG-CSD is an emerging low cost (low CAPEX-ultrafast growth) route to nanocomposite CCs with preformed nanoparticles
- We need to follow systematic studies of modifications of vortex pinning landscapes with irradiation using well stablished methodologies: ICMAB is open to collaborate in this challenge!

Acknowledgements

- Prof. Teresa Puig, Head Dpt.
- Members of Superconducting Materials and Large Scale Nanostructures (SUMAN) Dpt.
- Many PhDs and postdocs during the last 20 years